MASTER THESIS REPORT

FEM MODELLING, TESTING AND VALIDATION OF INDUSTRIAL ADHESIVE FOR AUTOMOTIVE APPLICATONS

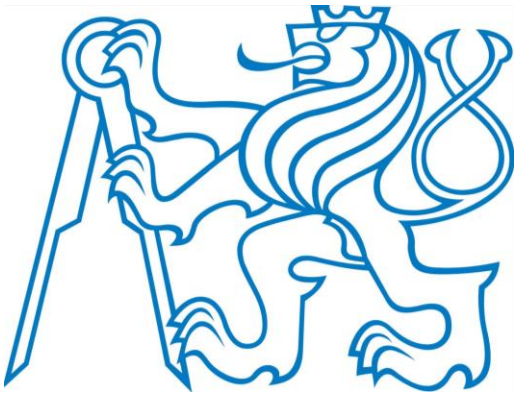

ČESKÉ VYSOKÉ UČENÍ TECHNICKÉ V PRAZE

PROBLEM OWNER: ING. JAKUB JELINEK (TÜV SÜD s.r.o.)

SUPERVISOR: ING. MICHAL VAŠÍČEK, PH.D. (ČVUT)

WRITTEN BY: AMAN BAHODIA

MASTER'S THESIS ASSIGNMENT

I. Personal and study details

Student's name: **Bahodia Aman** Personal ID number: **441659**

Faculty / Institute: **Faculty of Mechanical Engineering**

Department / Institute: **Department of Automotive, Combustion Engine and Railway Engineering**

Study program: **Master of Automotive Engineering**

Branch of study: **Advanced Powertrains**

II. Master's thesis details

Master's thesis title in English:

FEM Modelling, Testing and Validation of Industrial Adhesive used for automotive applications

Master's thesis title in Czech:

MKP modelování, zkoušení a ověřování průmyslových adheziv používaných v automobilních aplikacích

Guidelines:

To study and investigate different types of adhesives and get well versed with their structure and important properties (mechanical properties, rupture, failures, etc.)
To choose a specific brand and its adhesive based on the literature study as required.
To select and specify the physical tests to be performed with the selected adhesive.
Perform physical tests with the chosen adhesives and document all the test data.
To make FE material model of the adhesive on FE software PAM-CRASH.
To perform the simulation of the physical tests previously performed.
To validate the adhesive material model by correlating the physical test results and the simulation data.

Bibliography / sources:

Name and workplace of master's thesis supervisor:

Ing. Michal Vašíček, Ph.D., Department of Automotive, Combustion Engine and Railway Engineering, FME

Name and workplace of second master's thesis supervisor or consultant:

Date of master's thesis assignment: **30.10.2018** Deadline for master's thesis submission: **04.01.2019**

Assignment valid until: _____

Ing. Michal Vašíček, Ph.D.	doc. Ing. Oldřich Vítek, Ph.D.	prof. Ing. Michael Valášek, DrSc.
Supervisor's signature	Head of department's signature	Dean's signature

III. Assignment receipt

The student acknowledges that the master's thesis is an individual work. The student must produce his thesis without the assistance of others, with the exception of provided consultations. Within the master's thesis, the author must state the names of consultants and include a list of references.

3/1/2019	Bahodia.
Date of assignment receipt	Student's signature

PREFACE

This project was conducted as a research for TÜV SÜD s.r.o. The project was carried out within the frame of TÜV SÜD and Czech Technical University in Prague.

The purpose of this report is to present it as a master thesis project at Czech Technical University in Prague. The report is based on the work done on industrial adhesive. The report gives in depth insight of the work done during the six months project. The project's objective is FEM modelling, testing and validation of industrial adhesive for automotive applications.

The report should enable the reader to understand the physical model, the finite element model of the adhesive, the types of validation tests and simulations done for the project. This will also help other aspiring researchers and students to take it to next step and tune the adhesive material model using different material types, and/or for different adhesives.

Aman Bahodia

Prague, January 2019

ACKNOWLEDGEMENT

The project would not be successful without help and support of many people. I would like to thank doc. Dr. Ing. Gabriela Achtenová and my project supervisor at TÜV SÜD s.r.o., Ing. Jakub Jelinek. Prof. Achtenová for her immense support and initiative to get me this project and Mr. Jakub Jelinek for his unending help and guidance throughout the research. Furthermore, I am thankful to my University supervisor for this project, Ing. Michal Vašíček, Ph.D. He supported my work throughout the project and gave me a direction to critically think about my decisions during the course of this project.

I am grateful to professor, Ing. Petr Vondrouš, Ph.D. for his guidance and help at University, in early stages of the Project and Ing. Tomáš Kramár for being a great help in the University Lab. Ing. Michael Zoubek showed a great interest in the project; he helped and guided me greatly for the physical testing preparation in the lab. I would also like to mention the support from Ing. Karel Doubrava, Ph.D. who helped carrying out the tests at the University Lab.

At last, I acknowledge my family, friends and all the loved ones for believing in me and supporting me during this project.

SUMMARY

TÜV SÜD Czech S.r.o. is a global testing, certification, inspection and training provider also based in Czech Republic. They are constantly working to improve and add tangible economic value to automotive industry.

Popular conventional joining methods like riveting, welding and bolting are widely used in Automotive Industry. They are till now the best solution available for joining needs of the two parts. However, these joining methods put extra stresses in the area around them and hence a better solution needs to be researched.

The use of resin-based adhesive for joining is promising. They show a satisfying behavior and further research was needed under full test conditions. At first, the ASTM standard tests were chosen for the physical testing of the adhesive. Then, the finite element (FE) material model of the adhesive was made to better match it with the physical adhesive counterpart. Then, the physical tests were simulated on FEA software PAM-CRASH. The validation and tuning of FE model was done using the physical testing data collected from the ASTM tests and adjusting the key parameters.

This research could be a base platform for aspiring research students to further study the behavior industrial adhesives and provide them with an understanding of choosing a suitable adhesive based on the key parameters. The adhesive FEM model can be used to simulate the behaviour of the any adhesive, provided, it is tuned accordingly. This will enable the FEA specialist to include this model in the finite element analysis of a full-fledged vehicle testing simulations.

TABLE OF CONTENTS

LIST OF FIGURES

LIST OF TABLES

1 INTRODUCTION

1.1 BACKGROUND

Current joining methods like bolting, welding and riveting offers a good solution to the joining needs of the automotive industry around the globe. These conventional methods are good, but they have many cons as well in terms of joint strength, reliability, and ease of operations.

Nuts and bolts have been around from the times of Romans or even 400 BC. It is evident that they might have developed the first screw made from bronze or silver. Most significant developments have been made in recent 150 years in terms of using modern day nuts and bolts. The use of nuts and bolts serve most of the purpose in everyday household items. The automotive industry uses it in abundance as can be seen on Figure 1 , the reason being, that they are easily available, and the industry can order them in bulk. Apart from that, they can be installed fast, and one doesn't require special education or skill to use them. Bolting doesn't require much space for the operation and hence can be installed on site, easily. One doesn't need to take the part to be bolted in some special environment which would be safer for the operator. One of the advantage is also that this is a non-toxic joining method and hence it is safe for the operator unlike other joining method that are discussed later. Life span of bolted joints are quite long and even after being discarded they can easily be recycled and reused. With so many pros this joining method has some cons as well. Producing them is a complicated and expensive process and the leave a high energy footprint on the environment. For joining two surface using bolting, it is required to first drill the surfaces. This drilling, creates a pinot of extra stresses over the area and hence later becomes the point of interest as it would be the weakest point of the assembly. They are prone to corrosion over time as can be seen in Figure 2. Even though the clamp force is high the stresses over the bolted area cannot be ignored.

Figure 1: Nuts and Bolts assembly in Vehicle

Figure 2: Rusted Nut and Bolt assembly [1]

Over the time for saving more time during manufacturing the OEMs are switching to riveting as an alternative to bolting as it improves the SMED (single minute exchange of dies) of manufacturing. History of use of rivets can be traced back to the times of 3000 BC [2]. One of the major issue with using bolting as a joining method is that it gets loosen over time in an environment which is prone to vibrations and we cannot afford that to happen in a vehicle, this will put the safety at risk for the driver and the passengers. An example of riveting assembly can be seen in Figure 3. Apart from that, bolting is good for only short clamp lengths and if we need to have a long clamp length we need to use riveting. Installing rivets is as easy as bolting and can be done on site, there is no need to take the part to some special environment and it can even be installed from one side if there is no access to the opposite side. Rivets don't have threads and hence they don't rotate loose because of vibrations. It is also a non-toxic method of joining. As rivets also make a hole in the clamping surfaces they accumulate extra forces on the joining area which is a point of concern. And as it is a permanent joint, it is not possible to remove it from the site and reuse it on some other location like nuts and bolts.

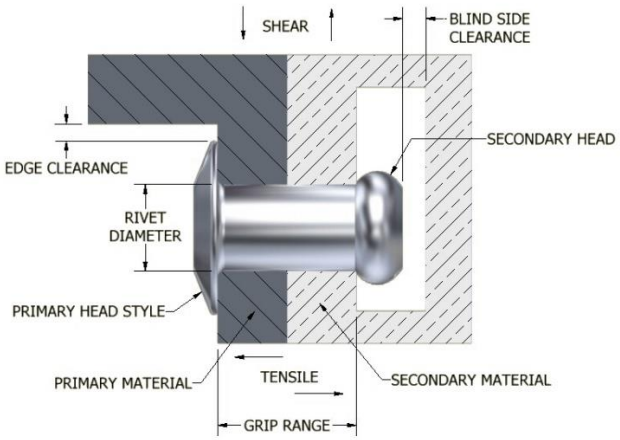

Figure 3: Riveting Assembly [3]

Welding, as method of metal fabrication has been around for a long time and its use can be traced back to Bronze Age when two metal samples were simply hammered to weld together. An example of welding in automotive industry can be seen on Figure 4. Conventional Welding, as we know it today, came into existence in 19th Century and it is advancing ever since. Over welding and other joining methods, it is a debate, which one is better. Automotive industry uses both the joining techniques as per their joining requirements and cost effectiveness. Welding operations are used mainly on the body B and frames. As welding provides a better finish while providing equally stronger joint, it makes a perfect choice when it comes to weld surfaces. Welding is highly automated in recent times and used in abundance as well for the same reason in automotive industry.

Figure 4: Example of Welding in Automotive Industry

The cost of bolting has decreased over the years, whereas the cost of welding is stable. It also depends on what kind of steel is used, for example galvanized or non-galvanized. Galvanized steel is rust-proof, but it also produces toxic zinc fumes while welding and hence the welding operation needs to be performed in controlled environment. It is not safe to perform overhead welding operations as there is chance of operator to get injured from the molten metal.

History of adhesives dates back to 70,000 BC, when caveman used a gluey substance made of tree-sap and red ochre to protect cave paintings [4]. Rubber based adhesives have been around for a long time and can be dated back to 1830. Earlier civilization depended more on adhesives made from plants, animal hides, connective tissues, hooves and heat-treated rubber substances. Resins were used to preserve the remains of the rich and royal families in Egypt.

Resin based adhesives have proven their reliability over time by preserving those remains for thousands of years. Resin based adhesive have also find their use in recent times, from metals, synthetic fibers, plastic films. Aerospace industry and automotive industry used these adhesives for many metal to metal bonding requirements. Figure 5 shows the application of adhesive in car body.

Figure 5: Application of Adhesive in Automotive Industry, [5]

The advantage of using adhesives is that they can be very reliable, long lasting, gives better finish, can be used on the places where other joining methods cannot reach because of space constraints and can they provide strong bonding strength to the joints, as there is no need to make a hole by drilling, like in the case of bolting and riveting, there are no extra stress points to weaken the bond. There are many types of adhesive, some are meant to be used directly and there is no need to prepare the solution. Adhesive used in industry are high quality and needs to bear more loading, these adhesives comes in more than one part, hence, there is a need to prepare them prior to application. Two-part, epoxy adhesives, needs special environment for application to avoid any contamination, also the mixing can be exothermic and special care needs to be taken during preparation. The bonding using adhesives is not instant but require a curing time. The duration, temperature, and moisture conditions for curing is described by the manufacturer.

1.2 PROBLEM DEFINITION

As mentioned earlier, TÜV SÜD is a certification firm that provides the safety certifications for the vehicle manufacturers. They specialize in physical as well as virtual crash test simulations for the same. As many manufactures uses adhesives on their products, it is crucial for TÜV SÜD to model all the joints as well in the PAM-Crash to get the realistic simulation results. Different joining methods can be modelled into PAM-CRASH, easily, using the predefined materials in the materials library.

The material model of the adhesive is not available in the library, but, can be modelled, by defining the parameters of the adhesive. The modelling requires the important parameter to be input, these parameters are usually not provided by the manufacturers and hence, needed to be evaluated. This evaluation can be done, by running some standard physical tests. The tests can be chosen from ISO or ASTM testing standards. These tests then can be simulated in the PAM-Crash environment and the material model can be tuned to match the physical tests. This approach can provide us with realistic and reliable adhesive model that can be used for certification simulations. Section 1.3 OBJECTIVES, describes the goals and their order, which were followed during this thesis work.

1.3 OBJECTIVES

1. To study and investigate different types of adhesives and get well versed with their structure and important properties (mechanical properties, rupture, failures, etc.).
2. To choose a specific brand and its adhesive based on the literature study as required.
3. To select and specify the physical tests to be performed with the selected adhesive.
4. Perform physical tests with the chosen adhesives and document all the test data.
5. To make FE material model of the adhesive on FE software PAM-CRASH.
6. To perform the simulation of the physical tests previously performed.
7. To validate the adhesive material model by correlating the physical test results and the simulation data.

1.4 LITERATURE SURVEY

To perform the physical testing and modeling the adhesive material model, it was necessary to get an insight of different types of adhesives, their properties and important parameters. Different modelling techniques were also looked at to get an insight for modelling.

Durability of Structural Adhesives [6] & Handbook of Adhesives and Surface Preparation: Technology, Applications and Manufacturing [7] gives knowledge about types of adhesive, important properties and surface preparation processes. This knowledge is applied to during the initial phase of the project for surface preparation for physical testing. ASTM and ISO standard tests were studied, and the tests were chosen to be performed. ASTM D1002 [8], ASTM D1876 [9] and ASTM D3528 [10] were chosen and performed as they were planned to be simulated in FE environments to tune and validate the adhesive material model.

Michal Zeleňák et al. [11] and Adnan Akkurt [12] gives an insight to different cutting methods available and their advantages and disadvantages. Based on their finding, material thickness and the requirements of test, shearing as cutting method has been chosen and is discussed in section 2.4.1 CUTTING PROCESS. To diagnose the oil and other contaminants, many different methods were studied, surface energy analysis [13] and infrared light oil detection method [14], followed by researching about degreasing [15] and abrasion methods for the samples. A suitable adhesive was chosen after researching different adhesives available and used in industry. Loctite EA 9466 was chosen, and its datasheet [16] was studied for important characteristics like Young's Modulus, Density, and curing time was studied and applied for the bonding and curing. These parameters were also used to define material model card for adhesive.

Many research, and findings were studied to find the solution for modelling the adhesive. L. F. M. da Silva et al [17] studies three different methods for adhesive modelling, Finite Element method, Boundary Element method and Finite Difference method and found that FE method, although needs more research, is more suitable to model adhesive. Whereas, BE method is still in development and FD method is useful for solving differential equation derived in complex analytical models.

Ficarra 2011 [18] discusses about peel stress and shear stress distribution in adhesive layers, elastic-plastic behavior of modern adhesives and gave motivation to use elastic-plastic material card while modelling the adhesive material model. It als describes the different surface pre-treatment like sanding and acetone. And typical failure in single lap joints. Many of the research findings like choosing sanding and degreasing over acetone and deciding adhesive material card to model adhesive has been used for the project.

Jakub Korta et al [19] talks about cohesive zone modelling and its advantages and got promising results. Andrea Spaggiari [20] studied two different modelling approaches to model adhesive material, Full FE model and Tied Mesh (TM) model. The study concluded that the TM modelling method is as efficient as the Full FE model, it produces accurate results and takes even significant less calculation time. A similar approach using tied contact is used for modelling the adhesive material, discussed in Section 3 FE MATERIAL MODELLING.

1.5 ADHESIVES, TYPES AND THEIR IMPORTANT PROPERTIES

A material which when applied to surfaces of materials can join them together and provide good resistance for separation is known as *adhesive*. Structural adhesives used in industry are based upon monomer composites which polymerize to give high-modulus, high-strength adhesives between relatively rigid adherends to construct a load bearing joint [6].

There are many kinds of adhesives available that are used in industry like resin, hot-melt, acrylic, anaerobic adhesive, conductive adhesive, pressure adhesive and epoxy adhesive. Structural adhesives are usually low molar mass phenolic, epoxy resin or acrylic resins. Acrylics resin-based adhesives have gained popularity for sufficiently low viscosity to flow over substrate surface without any aid from solvents. These are polar materials and assists in removing atmospheric contaminations and increase the degree of intrinsic adhesion. They polymerize to give highly crosslinked adhesives like thermosetting polymers.

Epoxy resins need curing agents (hardener) to set. Upon curing, they form a high degree of crosslinking, high-strength, low creep behaviour, high-modulus and good elevated temperature properties. Inclusion of rubber, phase separates when resin is cured gives it a two-phase microstructure which makes it resistant to its expected brittle nature.

It has been found that an intimate molecular contact at the interface is necessary, for a strong adhesive joint. Adhesive should spread over the adherend surface and should displace air or any other contamination from the surface. To find the nature of intrinsic forces acting across the interfaces to prevent separation, many different theories have been proposed.

The four main popular theories of them are, mechanical interlocking which proposes that interlocking of the adhesive into the irregularities of the substrate surface causes them to adhere; diffusion theory states that the adhesion is caused due to mutual diffusion of polymer molecules across the interface; electronic theory suggests that adhesive and substrate have different energy band structures and upon contact there is transfer of electron to balance of Fermi levels which will result is forming of double layer of electrical charge on the interface; and finally the most accepted theory of adsorption suggests that the materials bonds due to

surface forces acting between the atoms of the two surfaces and are called as van der Waals forces, in addition to that ionic, covalent and metallic bonds may operate across the interface as well. The important mechanical properties to determine the quality of the adhesives are as follows:

- Young's modulus of elasticity,

$$E = \frac{Stress}{Strain}$$

Equation 1: Young's Modulus of Elasticity

- Shear modulus,

$$G = \frac{E}{2(1+v)}$$

Equation 2: Shear Modulus

- Bulk Modulus,

$$K = \frac{E}{3\,(1-2v)}$$

Equation 3: Bulk Modulus

- Poisson's ratio,

$$v = \frac{d\varepsilon_{trans}}{d\varepsilon_{axial}}$$

Equation 4: Poisson's Ratio

Where, ε_{trans} is transverse strain and ε_{axial} is axial strain.

These parameters define the behavior of the adhesive under shear loading. They parameters were crucial when modelling the material model of adhesive in Section 3.1 MODELLING. Figure 6 shows typical stress-strain behavior of different types of adhesives.

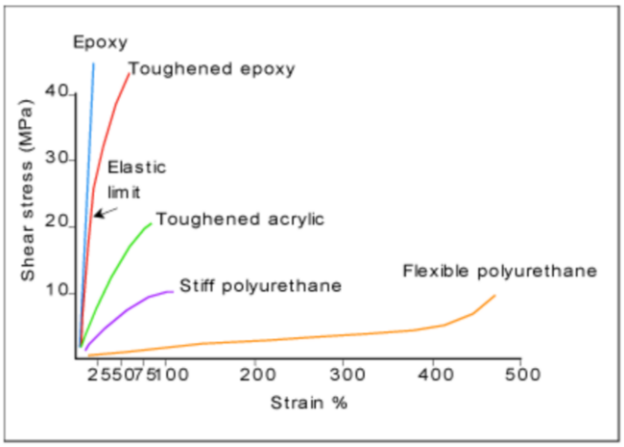

Figure 6: Stress - Strain Behavior of Different Types of Adhesives [21]

Failure of the adhesive joint depends on the multiple factors, but the main factor is contact of the joint with water (liquid or vapor). Presence of water in the environment of the joint is the most harmful and most commonly diagnosed factor. Adhesive are designed to perform under a certain range of temperature and if they are pushed to their limits they tend to lose their joint strength and ultimately fail. Epoxy adhesives are preferred as they are popular for their superior joint durability and lower cure temperature and pressure requirements.

The material of the adherends also plays an important role in the durability if the joint. Metallic adherends tend to form oxides on their surface and makes the joint weaker. Quality of pre-treatment of the adherend is also an important factor. It is also observed that rate of loss of joint strength will be faster if the joint tensile or shear stress is present. Adhesive shrinkage or swelling also causes to form internal stress in the joints, making it weaker. At last the design of the joint is also a vital player in determining the joint strength. Standard peel test is more susceptible to environmental attacks than the lap joint.

2 PHYSICAL TESTING PREPARATIONS

2.1 SELECTION OF STANDARD PHYICAL TESTS

Selection of the physical testing is a crucial step as the material modelling is validated based on these tests. There are many tests available in both ISO and ASTM standards for this task. There are many methods to test the durability of the adhesive joints, some examples can be seen in Figure 7. The durability of an adhesive is usually measured in terms of its lap shear strength. Doing a lap shear test is ideal for the same. Apart from that peel test and double lap shear strength tests are also feasible for an in-depth study of the behaviour of the adhesive under peeling and double lap shear testing.

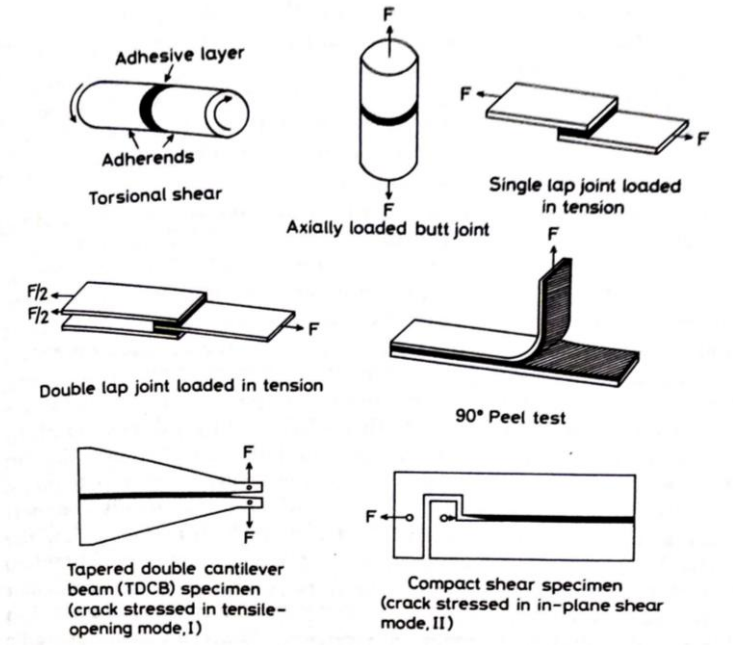

Figure 7: Different Tests to Assess Durability of Adhesive Joints [6]

In ASTM standard tests ASTM D1002 is a test designated for guiding in lap shear testing. ISO 4578 is the test for lap shear test in ISO standards. Similarly, ASTM D1876 and ISO 11339 are the tests for peel tests in ASTM and ISO standards. And ASTM D3528 is test guidelines for double lap shear testing. The choice of performing ASTM tests were made since the ISO test guidelines for double lap-shear test are not available.

2.1.1 ASTM D1002 [8]

ASTM D1002 describes in detail about the test procedure. It includes the different grades and type of materials that can be used for the test. It also gives the dimensions of the specimen that are to be followed for the test. The test method finds application in controlling parameters (surface preparation, primer and adhesive) that determine the strength properties of the tested systems. The normal variation is the factors like temperature and moisture in the working environment may cause the adherents and the adhesive to swell or shrink as they both have different thermal and moisture coefficients of expansion.

The testing machine should be capable of maintaining a rate of loading 80 to 100 kg/cm2 or the rate of loading should be set at 1.3mm/min. The jaws of the machine should grip the outer end of the specimen from each end firmly. The machine should be calibrated as such that the load applied is always along the center line of the grip assembly. Length of the specimen overlap can be varied as per necessity while the length of the specimen in the machine jaws must remain the same. The distance from the end of the jaw to the end of the lap should remain 63mm in all tests.

Materials A 109, A 167, B 209 are ideal for these tests, however, the selection of material is discussed in detail in section 2.2 (Selection of Material). The thickness of the material for the test should remain 1.62± 0.125 mm and the length of overlap should preferably be 12.7 ± 0.25 mm. The variation in thickness and overlap will likely influence the test values. However, the thickness of the material chosen is different for this test and it is discussed in section 2.2 (Selection of Material). Form and dimension of the test specimen as mentioned in the ASTM document can be seen in Figure 8.

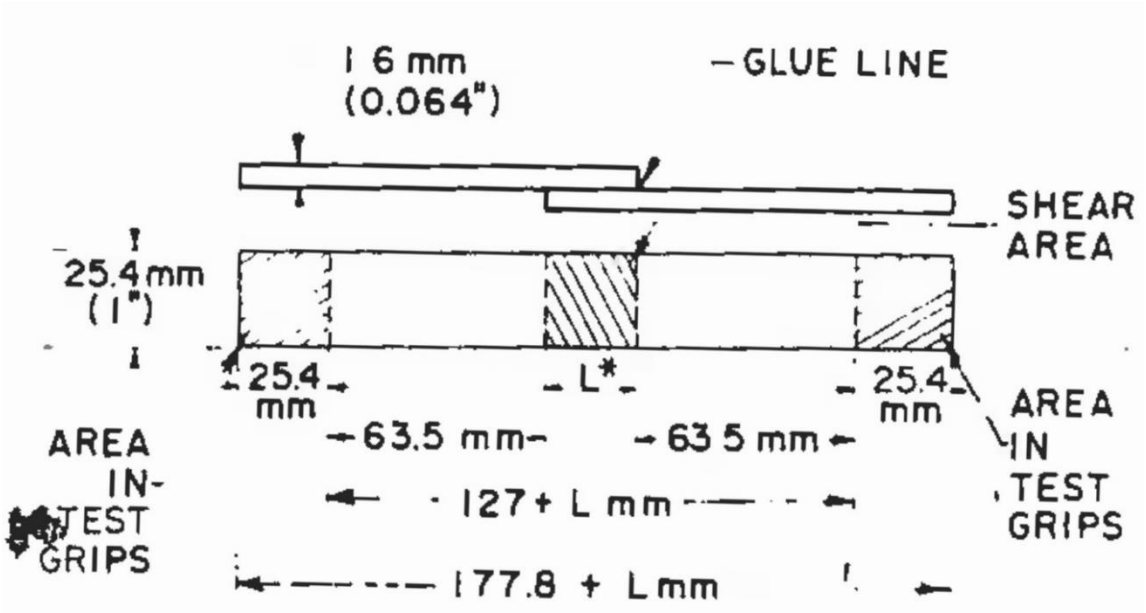

Figure 8: Form and Dimensions of Test Specimen ASTM D1002 [8]

The specimen is cut from the 1m x 2m sheets. Cutting was performed to avoid overheating or mechanical damage to the joint. After cutting, the surface was pre-treated for the adhesive application. Surface pre-treatment is discussed in the Section 2.4.2 (Surface preparation). Immediately after the surface pre-treatment the adhesive is applied so avoid the contamination of the surface due to oxidation if left unattended. The adhesive is applied, and two pieces were put together facing each other and the assembly is secured using clamps. The prepared batch of the specimen is put to special moisture and temperature-controlled environment for curing for a certain amount of time (details in Section 2.4.3).

2.1.2 ASTM D3528 [10]

ASTM D3528 describes in detail about the test procedure. It mentions the different grades and type of materials that can be used for the test. It also gives the dimensions of the specimen that are to be followed for the test. The test method finds application in controlling parameters (surface preparation, primer and adhesive) that determine the strength properties of the tested systems. The normal variation is the factors like temperature and moisture in the working environment may cause the adherents and the adhesive to swell or shrink as they both have different thermal and moisture coefficients of expansion similar to the other two tests performed.

The testing machine should so selected that the breaking load of the specimen lies between 15 -85 % of the full-scale capacity. It should be capable of maintaining a rate of loading 85 to 100 kg/cm2 or the rate of loading should be set at 1.27 mm/min. The jaws of the machine should grip the outer end of the specimen from each end firmly. The machine should be calibrated as such that the load applied is always along the center line of the grip assembly. Length of the specimen overlap can be varied as per necessity while the length of the specimen in the machine jaws must remain the same. The distance from the end of the jaw to the end of the lap should remain 63mm in all tests.

Materials A 109, A 167, B 209 are ideal for these tests, however, the selection of material is discussed in detail in section 2.2 (Selection of Material). The thickness of the material for the test should remain 1.62 ± 0.125 mm for 'B' type metal strips, 3.24 ± 0.125 mm for 'A' type metal strip and the length of overlap should preferably be 12.7 ± 0.25 mm as can be seen in Figure 9. The variation in thickness and overlap will likely influence the test values. The thickness of the material chosen is different for this test and it is discussed in section 2.2 (Selection of Material). Form and dimension of the test specimen as mentioned in the ASTM document can be seen in Figure 9.

Figure 10 shows an alternate form and dimension type for ASTM D3528 Double Lap Shear test. The decision of choosing one of the two types (1 & 2) was based upon the simplicity of the design and ease of bonding, clamping and curing. Type 1 out of the two fulfilled the criteria for simple design and ease of handling whole bonding and clamping and hence was chosen to go move forward with.

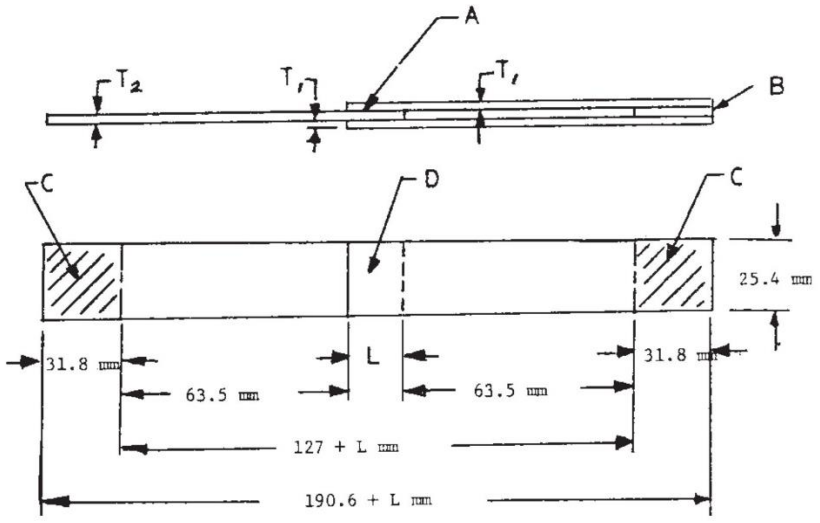

Figure 9: Form and Dimensions of Test Specimen Type 1, ASTM D3528 [10]

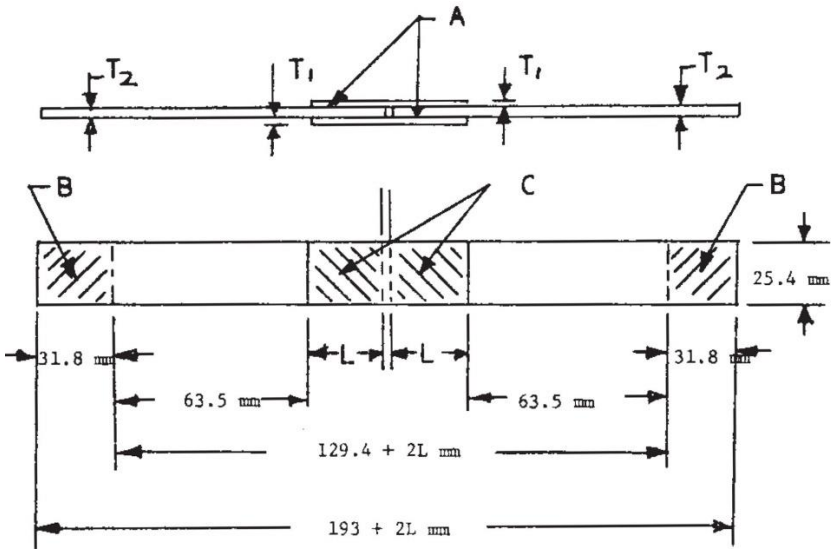

Figure 10: Form and Dimensions of Test Specimen Type 2, ASTM D3528 [10]

The specimen is cut from the 1m x 2m sheets of different thickness for this test as we had requirement of two different thicknesses. Shearing was performed to avoid overheating or mechanical damage to the joint. After cutting, the surface was pre-treated for the adhesive application. Surface pre-treatment is discussed in the Section 2.4.2 (Surface preparation). Immediately after the surface pre-treatment the adhesive is applied so avoid the contamination of the surface due to oxidation if left unattended. The adhesive is applied, and all the pieces were put together facing each other and the assembly is secured using clamps. The prepared batch of the specimen is put to special moisture and temperature-controlled environment for curing for a certain amount of time (details in Section 2.4.3).

2.1.3 ASTM D1876 [9]

ASTM D1876 describes in detail about the peel test procedure. As the other tests, it allows use of different grades and type of materials used for this test. It also gives the dimensions of the specimen that are to be followed for the test. The test method finds application in controlling parameters (surface preparation, primer and adhesive) that determine the strength properties of the tested systems. The normal variation is the factors like temperature and moisture in the working environment may cause the adherents and the adhesive to swell or shrink as they both have different thermal and moisture coefficients of expansion similar to the other two tests performed.

The machine and range should be selected so the maximum load o the specimen falls between 15 and 85% of the upper limit of the loading range. The jaws of the machine should grip the outer end of the specimen from each end firmly. The load should be applied at the constant head speed of 254 mm/minute. The machine should be calibrated as such that the load applied is always along the center line of the grip assembly. Length of the specimen overlap can be varied as per necessity while the length of the specimen in the machine jaws must remain the same.

Materials A 109, A 167, B 209 are ideal for these tests, however, the selection of material is discussed in detail in section 2.2 (Selection of Material). The thickness of the material for the test should remain 0.8 ± 0.125 mm the length of overlap should preferably be 241 ± 0.25 mm as can be seen in Figure 11. The variation in thickness and overlap will likely influence the test values. The thickness of the material chosen is different for this test and it is discussed in section 2.2 (Selection of Material). Form and dimension of the test specimen as mentioned in the ASTM document can be seen in Figure 11.

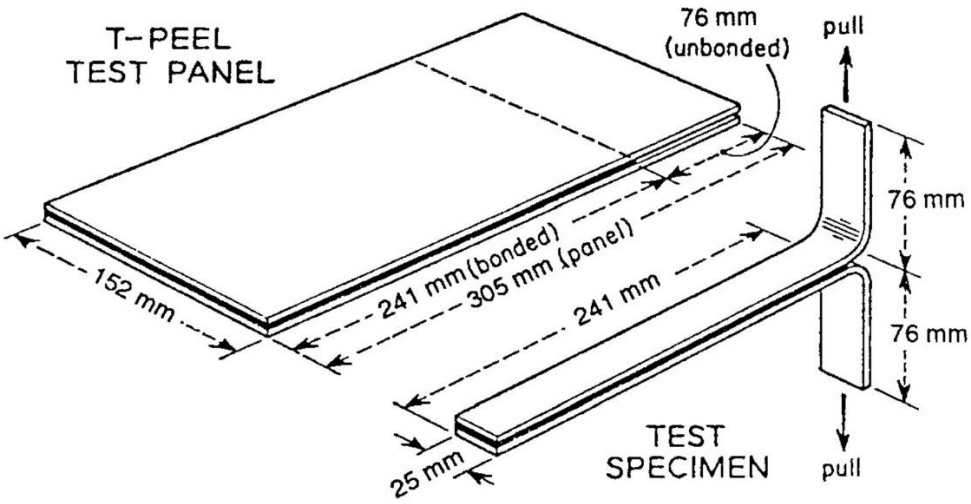

Figure 11: Form and Dimensions of Test Specimen, ASTM D1876, [9]

2.2 SELECTION OF MATERIAL

As mentioned in Section 2.1 SELECTION OF STANDARD PHYICAL TESTS, the ASTM documents gives a wide variety of materials like aluminum, brass, copper, titanium and steel to choose from. In automotive industry, the most common materials used for frame of the vehicles is usually aluminum and steel. Ideal would be to use one of the aluminum alloys type mentioned in the ASTM documents as these are the major consumed alloys for frames. Aluminum grades like B 209, alloy 2024, T3 temper could be used for the same. However, these grades are difficult to get in such small quantities and due to the lack of the suppliers for these grades of aluminum and particularly in the required thicknesses (0.8 mm, 1.6 mm and 3.2 mm). Aluminum grade 6061 T6 was also considered for the tests as other grades mentioned were not available. It was also not possible to get a hold on to any supplier that would provide it in the required thicknesses.

The choice of using steel grade S235JR for 3.2 mm and 1.6 mm thick sheets and EN 10130 DC01 for 0.8 mm thick sheet was made. These grades are easily available at the steel suppliers in Czech Republic and can be delivered fast. However, the thickness sheets of 1.5 mm were used instead of 1.6 mm and sheet of thickness 3 mm was used instead of 3.2 mm. Sheets of thickness 1.6 mm and 3.2 mm was not available at any supplier, hence the decisions on using the thickness closest to the mentioned in the ASTM were used.

KONDOR s.r.o. is a Czech Republic based steel supplier company and they could provide the steel sheets of the 0.8 mm, 1.5 mm and 3 mm thicknesses. The sheets of thickness 0.8 mm and 1.5 mm are cold-rolled sheets and the 3 mm sheets are usually hot rolled. The cold-rolled sheets are usually covered in a thin layer of oil and must be degreased properly during surface pre-treatment for proper wetting of the specimen surface. Hot- rolled sheet (3mm) is usually covered in oxides due to corrosive properties of steel and hence had to be blasted with suitable material during surface pre-treatment, discussed in more details in Section 2.4. Material for 0.8 mm thick sheet is EN 10130 DC01 as it is typical grade used for sheets thinner than 1.5 mm. S235JR is the material available for thicknesses 1.5 mm and 3 mm sheets. KONDOR S.r.o. supplied these sheets in sizes 1 m x 2 m for each thickness and the specimen were cut from these sheets using shearing. Cutting process is discussed in more details in Section 2.4.1 CUTTING PROCESS.

2.3 SELECTION OF ADHESIVE

There are many types of industrial adhesives available to choose from for these tests. This section discusses, in detail, about the available adhesives and the criteria kept in mind to choose a suitable adhesive for the ASTM tests. Based on the results of these tests, the chosen adhesive was modelled on FEA Pre-process software ANSA, then the tests were simulated on Pam-Crash and the results were validated using the Post-Processing software META.

Two-part epoxy adhesives are usually used in the automotive industry, hence the search for a suitable adhesive lead to the names like 3M, Sikadur, Loctite and Gurit. All these adhesive makers provide different type of adhesives based on application, conditions of use and the strength required out of the application. Loctite EA 9466 is an adhesive produced by Henkel. The adhesive is chosen It is a two-part epoxy adhesive with a 2:1 resin and hardener mixing ratio. Typical properties of 1.2 mm thick adhesive film cured for 7 days at 22℃ are given in the Table 1.

Physical Properties LOCTITE EA 9466	
Glass Transition Temperature	62 °C
Shore Hardness	60 Durometer
Elongation	3 %
Tensile Strength	32 x 10^{-3} GPa
Tensile Modulus	1.718 x 10^{-3} GPa

Table 1: Physical Properties of Loctite EA 9466 [16]

Figure 12 shows the items that assembles to be used for the application of the adhesive. The adhesive comes in a container with two chambers, one of each is dedicated to resin and hardener. The container can be installed in the applicator and the mixer attaches to the opening of the container. The mixer is designed, so that, the resin and hardener travel together in a zig-zag manner over the length of the mixer before being applied.

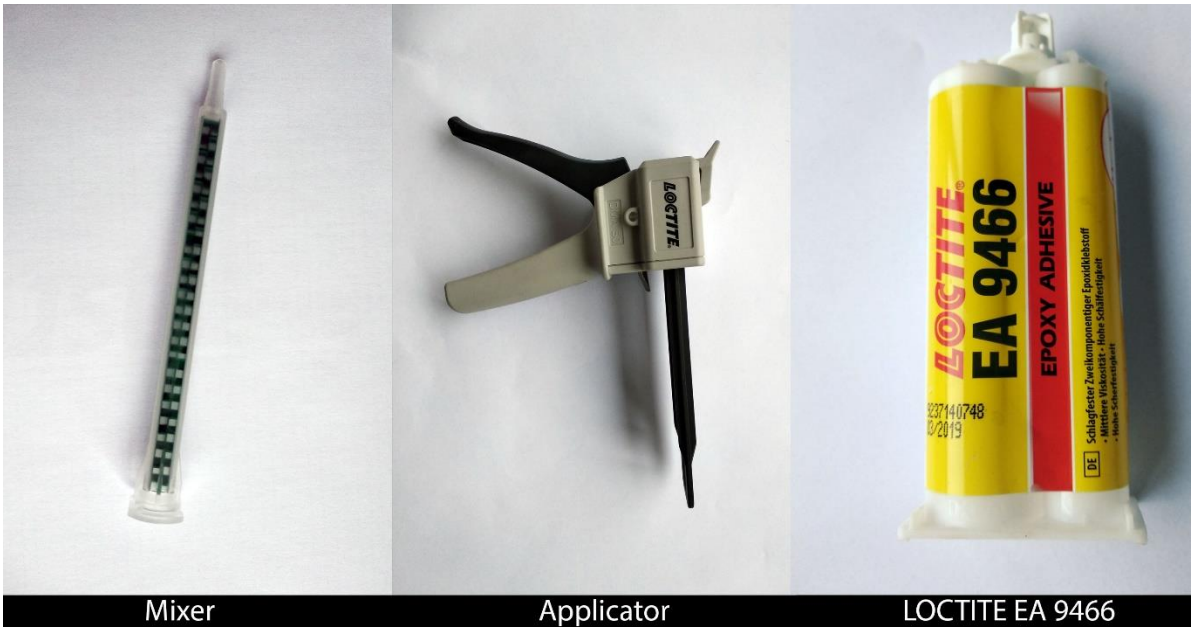

Figure 12: Loctite EA 9466 with Mixer and Applicator

2.4 SPECIMEN PRAPARATION

2.4.1 CUTTING PROCESS

Cutting of the steel sheets into the specimen sizes were a crucial step, as wrong cutting method chosen could destroy the structure and form of steel. Our goal was to make the specimen flat for the application of the adhesive. Using circular saw cutting method for the 0.8mm sheet would not have been a good choice.

Many methods like mechanical shearing, abrasive water jet cutting, milling, CO_2 laser beam cutting, plasma cutting, and oxygen flame cutting were studied. The cutting method was evaluated based on surface finish it gives to the surface, availability and the cost imposed. Michal Zeleňák et. el. [11] explains the differences in surface roughness of titanium samples undergone Abrasive water jet cutting and CO_2 laser beam cutting. Their findings suggest that the Abrasive Water Jet (AWJ) cutting produces lower values of *Ra* (Surface Roughness Parameter) than that of CO_2 Laser Beam (LBC) cutting. While the values of *Ra* remained under 12 µm, it varied from 5 to 40 µm for LBC for different transverse speed. Higher the transverse speed the lower the surface roughness in case of AWJ but for LBC it is opposite.

Adnan Akkurt [12], studies the surface properties of cut face obtained by different cutting methods for AISI 304 Stainless Steel. The article evaluated the different cutting methods based on many parameters like transverse speed, energy consumption, etc. It examines the microstructures of the cut face and concluded that different methods have different pros and cons. For our purpose (considering surface roughness) milling cutting was best suitable method as it produces the desired surface roughness and is cost effective than the other methods.

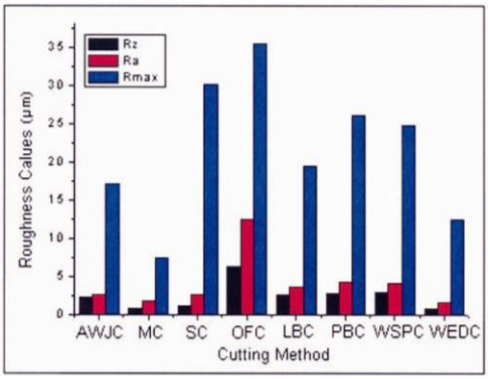

Figure 13 : Comparison of Roughness Values of Cut Faces Obtained By Cutting of AISI 304 Steel Material With Different Methods, Adnan Akkurt [12]

However, the process of milling every specimen by the edges would have been a very time and energy consuming process. It was important to have the surface roughness of a 5-6 µm of the working surface (bond faying surface). The edges are not the working surface; hence the adhesive would not be applied on the edges. The edges should be clean and burr free after the cutting process. Mechanical shearing was the perfect match for this and hence, the specimens were cut using mechanical shear machine from the 1 m x 2 m metal sheets.

Apart from cutting the metal sheets into specimen sizes, pieces of 31.8 mm and 25.4 mm were also cut from 1.5 mm and 3 mm thick steel sheets. The purpose of using these metal pieces was to serve as the spacer for clamping in the tensile loading machine cross head. This was done to make sure that the tensile loading during testing acts directly on the center axis of the glue line. Figure 14 shows the samples after cutting process.

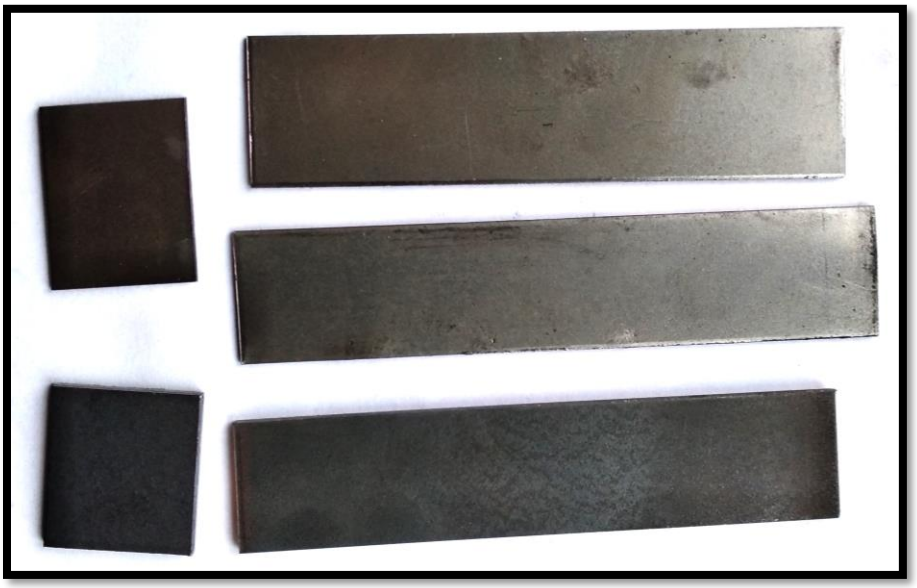

Figure 14: Samples After Cutting

2.4.2 SURFACE PREPARATION

The surface of the sheets needed to be prepared for glue application. The goal was to achieve a surface finish without any oil or oxides deposits on the surfaces as these impurities affect the quality of tests and hence their results. The sheets of thicknesses 1.5mm and 0.8mm are cold rolled and hence there are little to no chances for them to have any oxides deposits on their surfaces. However, the sheet with 3 mm thickness, is hot rolled and as a result in was bound to have oxides layer on its surface. In case of cold rolled sheets (0.8 mm & 1.5 mm), they generally have a layer protective oil over the surface. This layer of oil, needed to be addressed as well before we moved to the next step. Further, the bond faying surfaces needed to have a surface roughness between 5-6 µm.

Surface preparation was a process which needed diagnosis of oil and oxides on the surface, followed by degreasing, abrasion and again followed by degreasing before application of adhesive. For both the type of cold rolled and hot rolled sheets, the process differed because of the type of deposits on their respective surfaces.

There are many different methods available for diagnosing the oil film and oxides deposits on the surface of the sheets. One of methods involve using test inks. This method is used to determine the surface energy of the surfaces to be bonded. The ink is applied on the surface and it can be and checked if the ink applied change its form from being a line into droplets (can be seen in Figure 15, depending on that, the ink with higher or medium value of surface energy is applied. The surface energy is given by mN/m (milli-Newton per meter). Generally, the higher the surface energy of the surface, the better is the adhesion. The presence of grease, oil and finger print leads to surfaces having low surface energy. The other reason for a surface having low surface energy could be its material, Plastics, for example, have low surface energy and needs to be chemically treated prior to bonding.

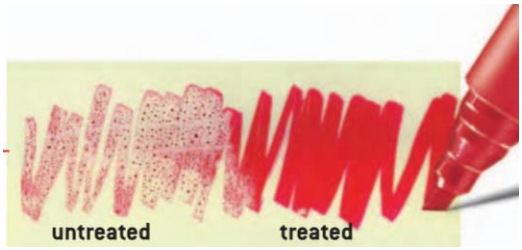

Figure 15: The difference between Surface energies of treated and untreated surfaces [13]

Another method uses a device called Recognoil, it is a surface contamination detector. The device provides the oil thickness and concentration on the surface and provides output in 2D and 3D. It can detect oil, grease layer as well as fingerprints. It principle of detection is based on the luminescence od the contaminants, the image is transferred to the computer software and analyzed. The device exposes the test sample to UV radiation (Figure 16) and while recording and evaluating the fluorescence of contaminants in the visible light spectrum.

Figure 16: Working principle of Recognoil [14]

Additionally, the software that come with the device, shows the high-resolution fluorescence map of contaminants distribution of the controlled area. The primary output provided is called as fluorescence intensity and is denoted by F.U. (Fluorescence Units). As metals generally do not exhibit Fluorescence, it is possible to detect the contamination levels of the metal surfaces. Figure 17 shows the typical output of the surfaces with three different contamination levels. As can be seen in the left most sample, the F.U. is 19506, which is very high contamination levels. The red area in the fluorescence map shows the presence of contaminants. The lower the F.U. value, the lesser is the contamination levels. The FU of the right most sample is 511, which is considered clean and ready to be used for adhesion purposes.

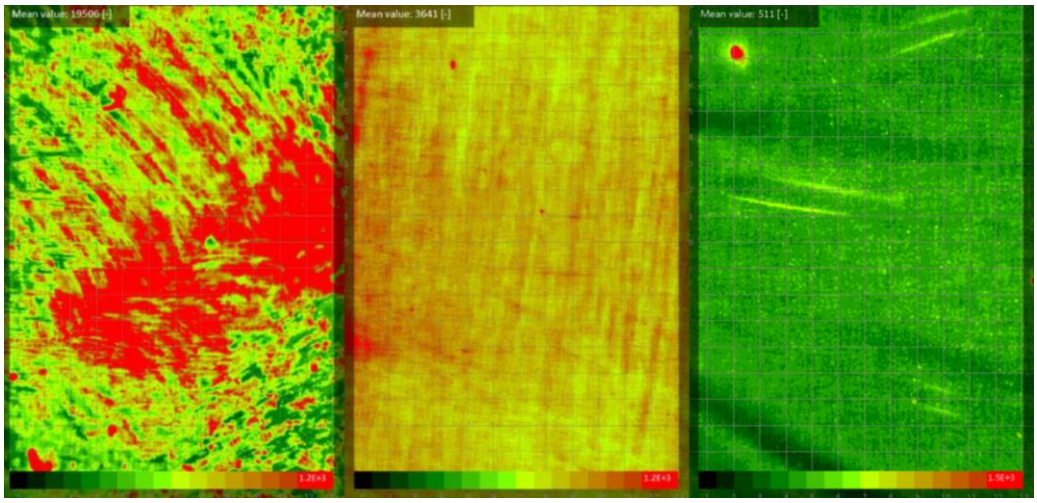

Figure 17: Examples of typical output of Recognoil 2W [14]

Recognoil was used for all the three surfaces prior to any treatment and at every step of surface pre-treatment leading to the bonding. Below, in Figure 18, are given the images of all three samples before any pre-treatment. The image shows that the cold rolled sheets (0.8 mm and 1.5 mm) have a thick film of oil and their corresponding F.U. are lying in the range of 23000 F.U. & 25000 F.U., while the 3 mm hot rolled sheet has a value of 315 F.U. because it has layer of oxides on it instead of oil.

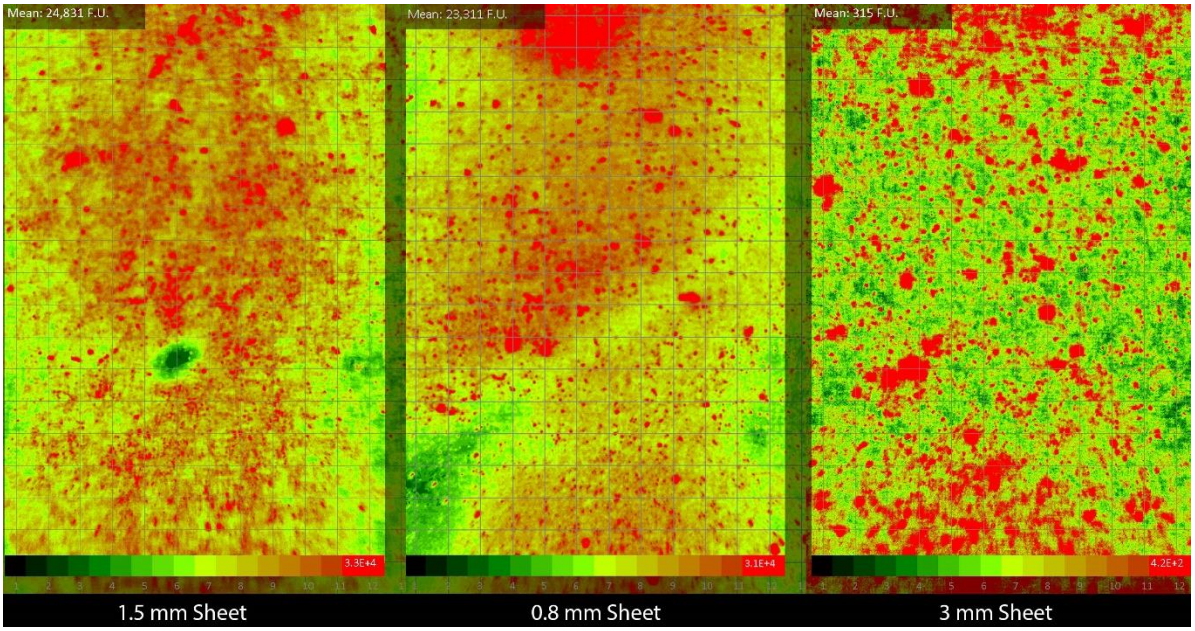

Figure 18: Fluorescence maps of three different samples before surface pre-treatment

As already discussed, 3 mm sheet being hot rolled, has oxides layer on its surface and to remove that, grit blasting was used. The setup for blasting the surface can be seen in Figure 19. The blasting machine uses the aluminum oxide grits of 80-100 grit sizes. Blasting was on both the sides of the samples and a matte-grainy finished was achieved, on the surface of the samples, after blasting. Method to check the size and quantity of dust particles of the blasted cleaned surfaces for painting or bonding, uses dust test kit. Dust test kit consists of adhesive tape, pictorial manual, and a comparator board to compare the samples for dust quantity and dust particle size.

Figure 19: Grit Blasting Machine

In the case of 1.5 mm and 0.8 mm sheets, blasting could have damaged the surface, hence, sanding them manually using a 160-grit sand paper was chosen as a method of abrasion. Sanding is necessary as it increases the bonding capability of the surface. Sanding removed the top layer of oil and the Recognoil results, as can be seen in Figure 20, shows a significant drop in F.U. for the case of 1.5 mm (4464 F.U.) and 0.8 mm (4117 F.U.) thick samples. However, for the case of 3 mm sheet the F.U. values increased to a higher value, the reason could be the contamination of the grits, for being used over the time, as the contaminants for the samples remains in the system and gets mixed. And hence, these contaminants can be transferred to the sample surfaces.

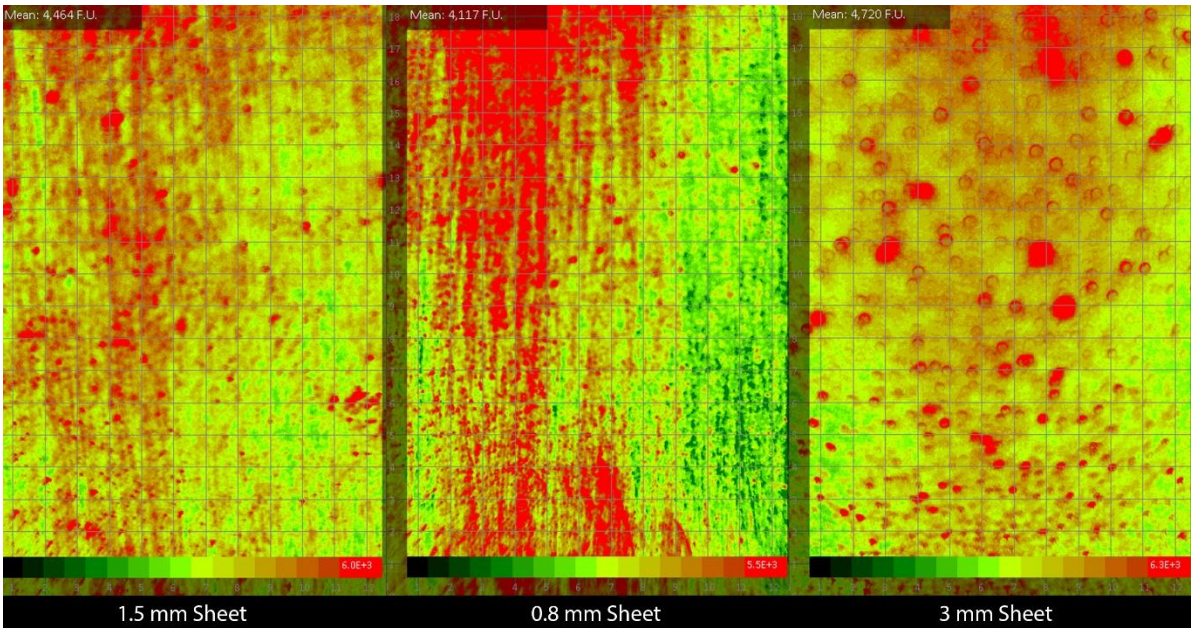

Figure 20: Fluorescence maps of three different samples after Abrasion

Next process in the surface pre-treatment was to degrease the samples and bring the F.U. further down. There are many different methods available for this task. Acetone is a well-known degreasing agent and is used in many applications where the surface is needed to be degreased. Typically, using Acetone, the samples are dipped in Acetone for a certain duration (2 hours) and then rinsed and then checked for contaminant levels and the procedure is repeated until the desired results are achieved. The drawback of using acetone is that, it is harmful for the user as it gives off the toxic fumes. Special care needs to be taken when handling. One must wear protective gloves and mask to protect from the fumes.

A safer alternative is to use the water-based degreasing agents. The process uses ultrasonic bath (Figure 21). The ultrasonic device is filled with 1:4 ratio by volume of degreasing agent and water. The device maintains a temperature of 40°C. Sanded samples are suspended into the bath and kept separated from each other. This is a quick method compared to acetone degreasing, as it only takes the device 10 minutes to complete one degreasing cycle. The samples are then checked for fluorescence units to check the oil layer on their surfaces. Figure 22 shows the fluorescence map of all the degreased samples. All the samples showed F.U. value less than 3000 F.U. and are degreased for bonding. This is achieved by 2-3 degreasing cycles of the samples.

Figure 21: Ultrasonic Bath and Degreasing Agent [15]

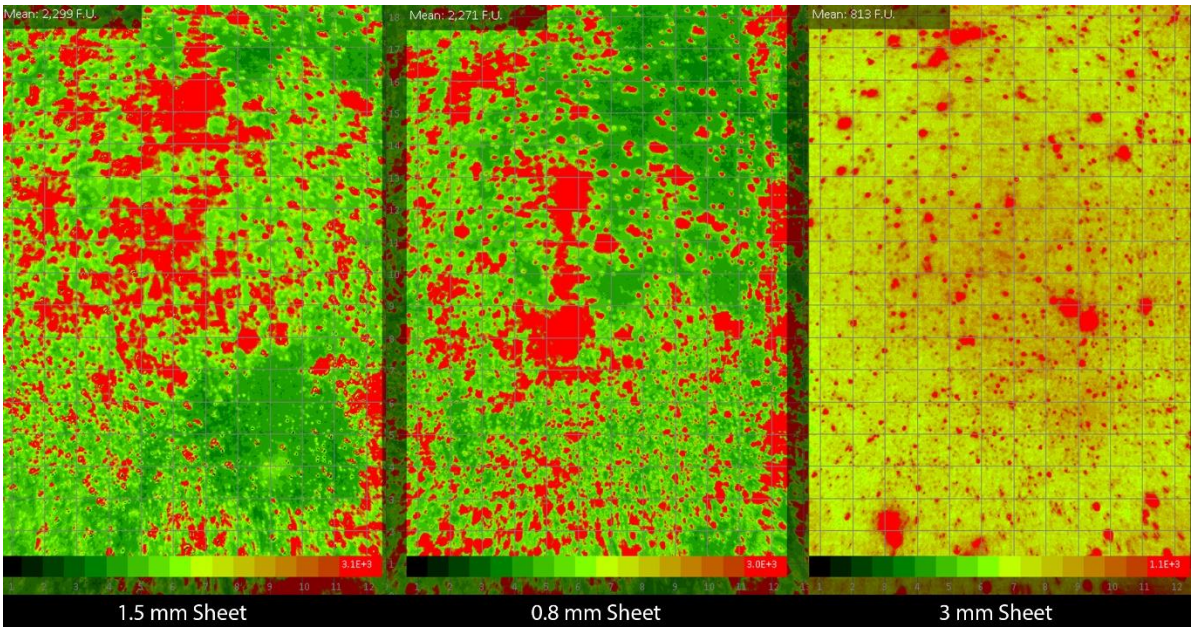

Figure 22: Fluorescence maps of three different samples after Degreasing

Surface roughness of all the samples were checked using portable surface roughness tester. The roughness of the bond faying surfaces, were under 6 µm.

2.4.3 BONDING AND CURING

After the surface of each specimen for all the tests were completed. The next task was to prepare the adhesive using the adhesive, applicator and the mixer as shown in Section 2.3. After surface pre-treatment, the specimens were wrapped in an inhibitor sheet to protect them from oxidation. These paper wraps were put inside an oxidation inhibition chamber. The samples were taken out one by one as and when needed. Special care was taken when handling the specimen, by wearing proper protective gloves, contamination of samples with oil and grease were avoided. The specimens were taken out as a set for the particular test and then marked 12.7 mm (ASTM D1002 and ASTM D3528 overlap length) and 241 mm (ASTM D186 overlap length). The adhesive was applied on the samples and it was made sure that the adhesive film thickness was even over the total overlap length. It was necessary to achieve the adhesive film thickness of 0.2 mm over the entire overlap length. Metal strips were put tightly together using clamps. Figure 23 shows one of the sample batch ready to be cured after clamping.

Figure 23 D1876 batch ready to be cured after adhesive application and clamping

Adhesive Loctite EA 9466, being used for the tests, comes with manufacturer's instruction for curing. There are different curing durations based on the temperature profile used. For a 1.2 mm thick film of adhesive with Steel, it can be cured for cured for 7 days at 22 °C. The strength achieved by curing in this condition can also be attained 100% by curing it at 40 °C for 6 hours or at 100 °C for 1 hour. Figure 24 shows the percentage of full strength of steel vs. cure time, temperature of the adhesive as mentioned in the manufacturer's datasheet [16]. Curing at 40 °C for 6 hours was chosen for our tests. For this, laboratory grade oven was used which can maintain temperature and humidity for extended periods of time.

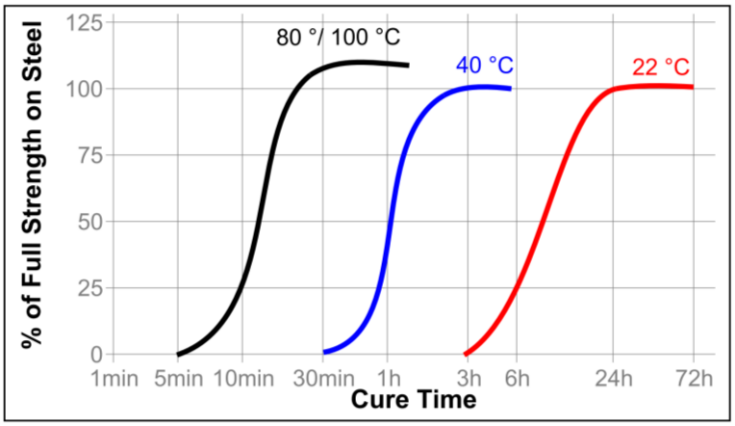

Figure 24: Percentage of full strength of Steel vs. Cure Time, Temperature Loctite EA 9466 [16]

Figure 25 shows the cured samples. The figure also indicates the use of spacers in both the D1002 and D3528 specimen.

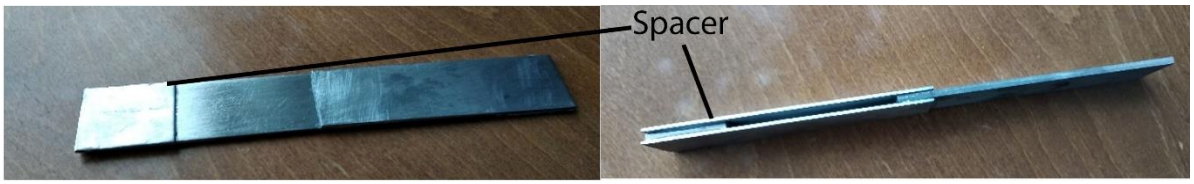

Figure 25: Cured Specimen Samples

2.5 PHYSICAL TESTING

The next step after bonding and curing was physical testing. The ASTM test documents mentions that, the machine should be able to maintain a rate of loading of 80 – 100 kg/cm2. The tensile machine shown in Figure 26 is a 100 kN machine and was capable to fulfil the loading requirements mentioned in the ASTM documents.

Figure 26: Tensile Loading Machine

The machine shown in Figure 26, can be used for tensile as well as compressive loading. The jaws were set according to the dimensions of specimen samples of each test. It was made sure that, the specimen is held exactly at the center of the grips, this ensured a symmetrical loading and minimized the risk of slipping of the specimen during the tests. For ASTM D1876 test the jigs were replaced with smaller sized jaws, as the unbonded part of the specimen was bent into a T shape (can be seen in Figure 11) and was not long enough to reach the center of the grips.

2.5.1 ASTM D1002

The specimens were marked and measured for glue line thickness. The glue line thickness varied from 0.18 to 0.22 mm for the 6 specimens prepared. The average glue line thickness came out to be 0.2 mm. This is very crucial to identify, as it played a major role in modelling the FEM model of the adhesive and setting up the virtual FEA simulations, in the later stages of the project. Figure 27, shows all the specimens numbered to be tested and the one of the samples mounted of the test grips to be tested.

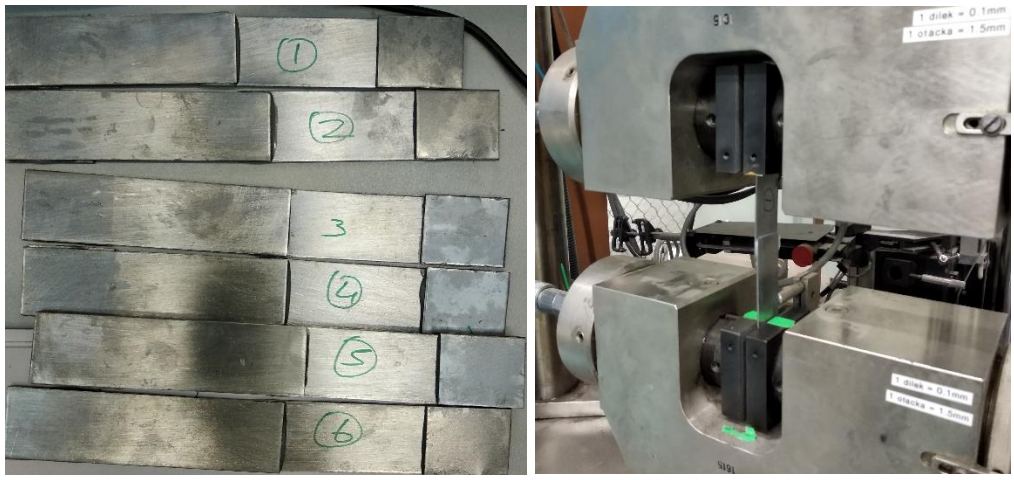

Figure 27: ASTM D1002 Physical Testing Batch and Testing Setup

Tests was carried out and the force against displacement were measured by the machine with the help of data acquisition system. At the point of failure, the samples were removed carefully, and the type of failure was assessed based on visual inspection. As can be seen in Figure 28, the rupture is partly cohesive and partly adhesive in nature.

Figure 28: ASTM D1002, Type of Failure Inspection

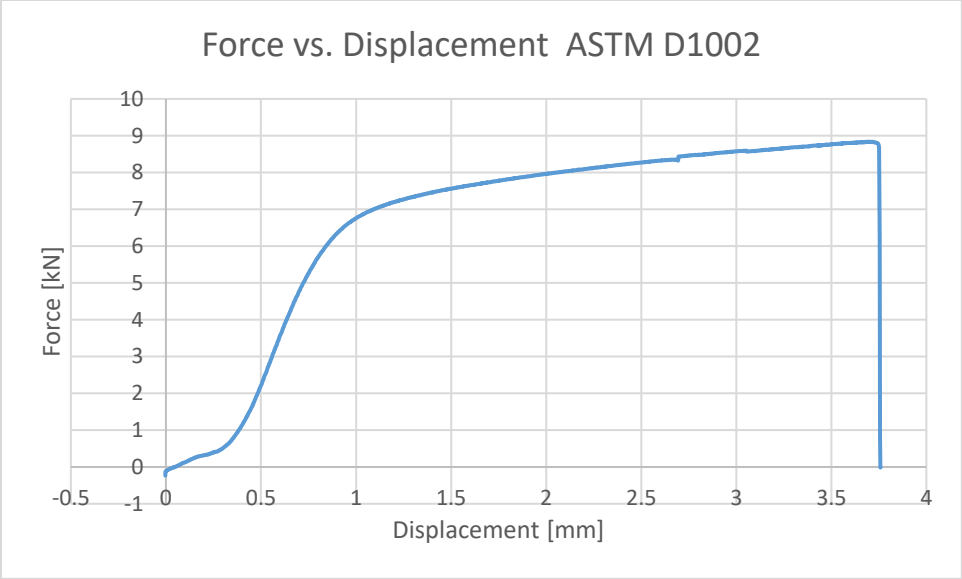

Figure 29: The Averaged Force vs. Displacement Curve for ASTM D1002

The Figure 29 shown above is the curve obtained by averaging the force vs. displacement curves of six different readings from the test. As can be seen, the maximum force after which the failure occurs, and the two plates gets detached is 8.83 kN force. At this maximum force, the displacement of the crosshead of the machine is at 3.7 mm. At this point, the adhesive has reached its failure limit and is ready to be ruptured. As the displacement of crosshead increases further, the force starts to drop drastically, and the material starts to detach. The cross-head stops moving as soon as the material is detached completely. Figure 30 shows the failure point of the specimen when the adhesive material is completely detached.

Figure 30: Failure of ASTM D1002 Specimen

2.5.2 ASTM D3528

The same process was repeated for this test. The specimens were marked and measured for glue line thickness. The glue line thickness varied from 0.18 to 0.22 mm for the 7 specimens prepared. The average glue line thickness came out to be 0.2 mm. Figure 31, shows all the specimens numbered to be tested and the one of the samples mounted of the test grips to be tested.

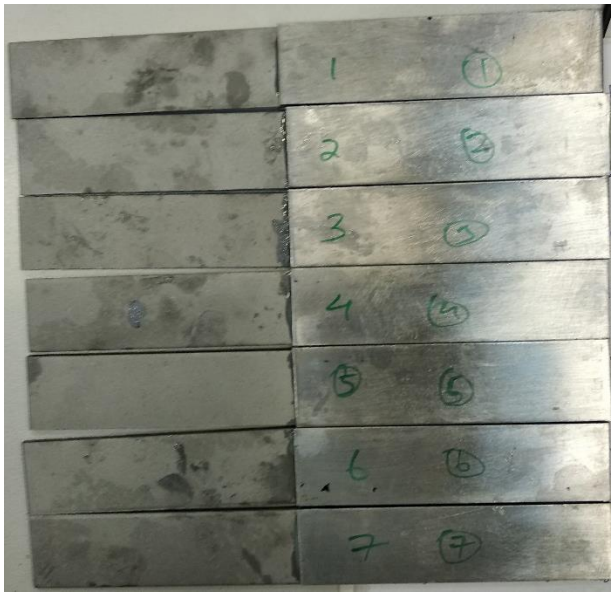

Figure 31: ASTM D3528 Physical Testing Batch

Tests was carried out and the force against displacement were measured by the machine with the help of data acquisition system. At the point of failure, the samples were removed carefully, and the type of failure was assessed based on visual inspection. As can be seen in Figure 32, the rupture is partly cohesive and partly adhesive in nature like ASTM D1002 tests.

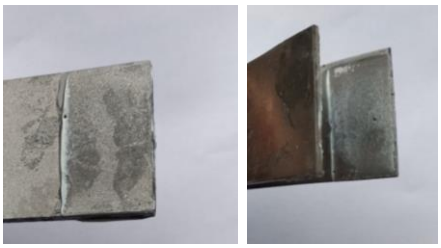

Figure 32: ASTM D3528, Type of Failure Inspection

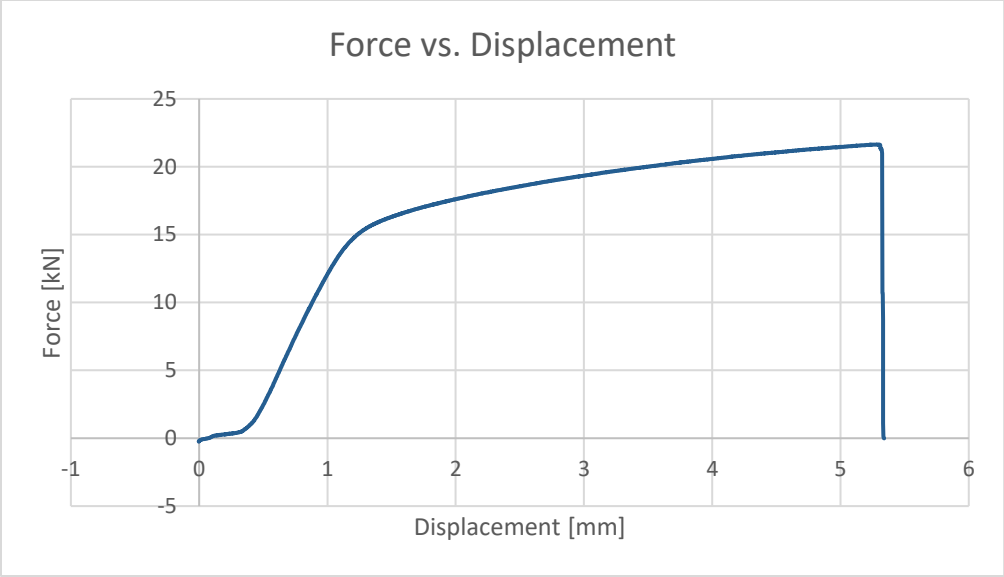

Figure 33: The Averaged Force vs. Displacement Curve for ASTM D3528

The Figure 33 shown above is the curve obtained by averaging the force vs. displacement curves of seven different readings from the test. The behavior of the adhesive force rise during the first 0.5 mm displacement in Figure 29 & Figure 33 can be justified by the fact that it takes a time for the grips to adjust and build up the force and this behavior is slip. As can be seen, the maximum force after which the failure occurs, and the two plates gets detached is 21.64 kN force. At this maximum force, the displacement of the crosshead of the machine is at 5.3 mm. At this point, the adhesive has reached its failure limit and is ready to be ruptured. As the displacement of crosshead increases further, the force starts to drop drastically, and the material starts to detach. The cross-head stops moving as soon as the material is detached completely.

2.5.3 ASTM D1876

As already discussed earlier, the setup of this tests was different compared to the other tests. Due to space constrains and size restrictions, smaller jaws needed to be used. After setting up the smaller grips the same procedure was repeated like the last two tests. All the seven samples were measured for glue line thickness. The average glue line thickness came out to be 0.2 mm, as desired. The machine was calibrated, as such that, the load applied was always along the center line of the grip assembly. Figure 34 shows the typical test setup for Peel Test.

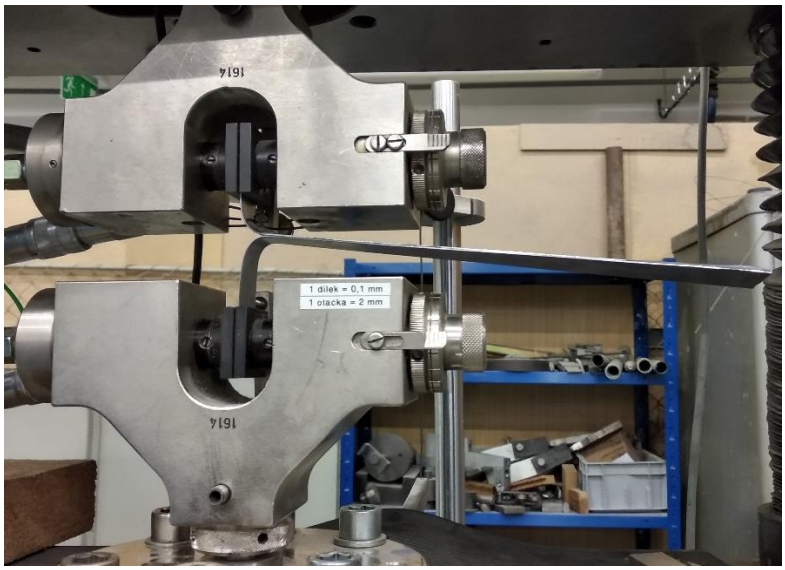

Figure 34: Typical Test Setup for ASTM D1876

Tests was carried out and the peel force against displacement were measured by the machine with the help of data acquisition system. At the point of failure, the samples were removed carefully, and the type of failure was assessed based on visual inspection. As can be seen in, the rupture is partly cohesive and partly adhesive in nature.

Figure 35: ASTM D1876 Peeled Specimen Visual Inspection

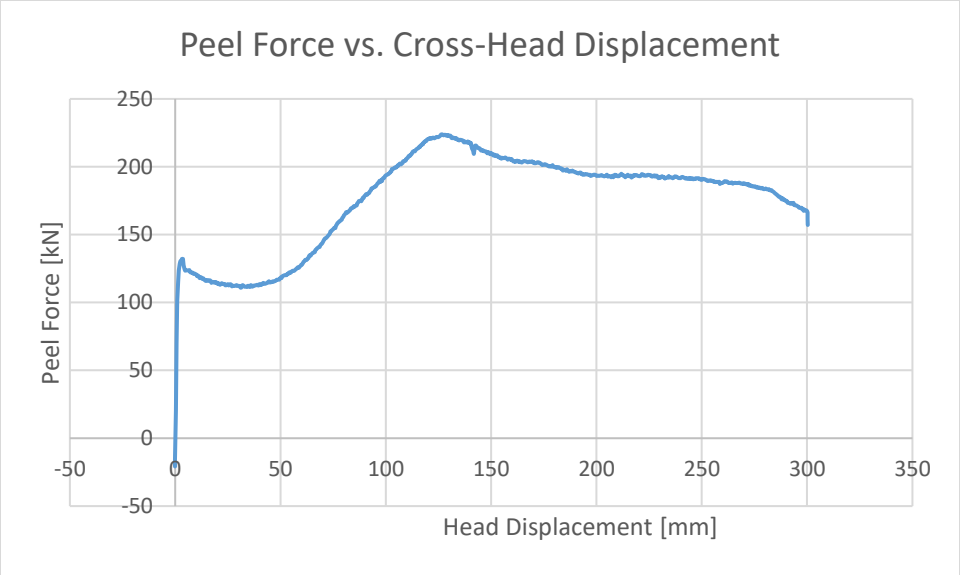

Figure 36: Peel Force vs. Cross-Head Displacement for ASTM D1876 Test

The peel force was measured for 300 mm of cross-head displacement. Figure 36 Shows the averaged curve for the seven test readings for ASTM D1876.

3 FE MATERIAL MODELLING

3.1 MODELLING

The modelling of the tests was done on the pre-processor ANSA for PAM-CRASH. The software is capable of modelling 3D objects using shell and solid elements. Table 2 shows the units of the parameters being used in ANSA and META (post processing software).

Measurements	Units
Length	mm
Time	ms
Mass	kg
Force	kN
Pressure	GPa
Young's Modulus of Steel	210
Density of Steel	$7.85 * 10^{-6}$
Gravitation	$9.81 * 10^{-3}$

Table 2: Unit System followed in ANSA and META

At first, the points were created in the 3D space, as per the dimensions of the specimen for all the three ASTM tests. The points were connected using lines and the surface was generated (Figure 37). On this surface, the meshing was done. The goal was to create a quadrilateral mesh and avoid triangular mesh elements, as they have shear locking tendency. Quads behave better in bending conditions compared to triangular elements. Figure 38 shows mesh for all the test setups. The mesh created in the intended overlap region was finer than the rest of the area on the plates. The finer mesh gives us better insight of the forces and the calculation is more accurate and detailed. However, it is not feasible to make a fine mesh over the whole plate as it would increase the calculation loan and hence, the calculation time of the simulation.

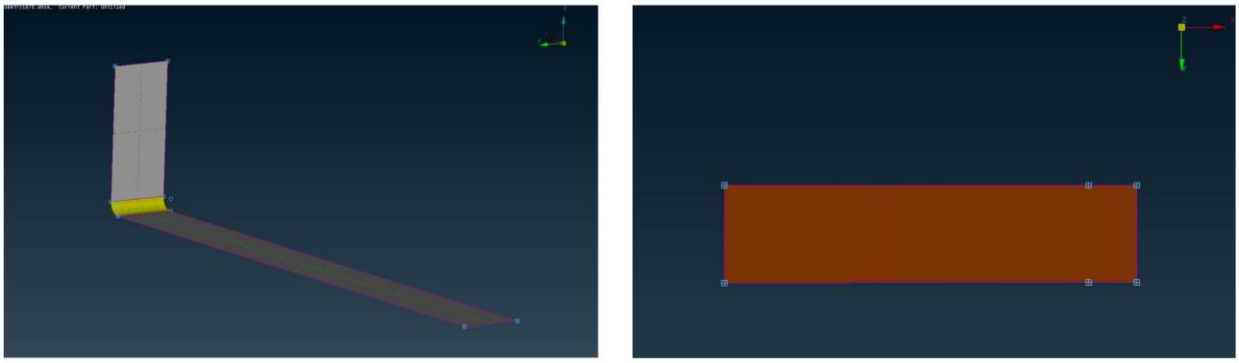

Figure 37: Points & Lines in 3D space on ANSA for D1002 and D1876

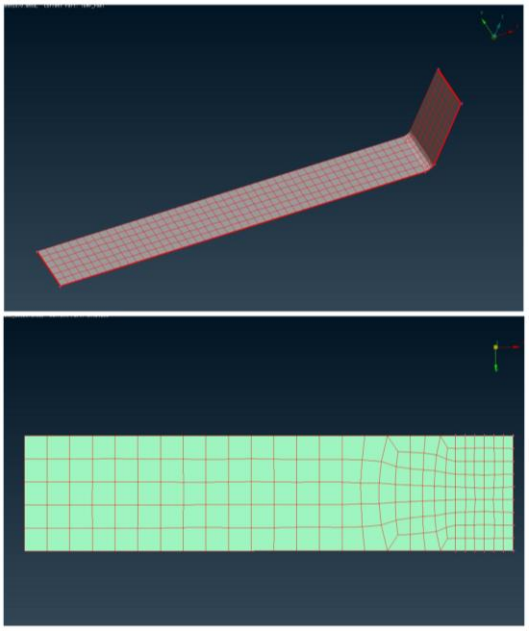

Figure 38: Mesh for ASTM D1002, D3528, D1876

The solids were created using '*extrude*' command from the meshed surface. The thickness depends on the respective tests they were created for, 0.8 mm for ASTM D1876, 1.5 mm for ASTM D1002, 3 mm & 1.5 mm for ASTM D3528. The Extrude command creates solids perpendicular to the meshed surface in the specified direction. The solids created is already meshed because the surface was meshed prior to extruding. Figure 39 Shows an example of solids created using Extrude command for ASTM D1002 test.

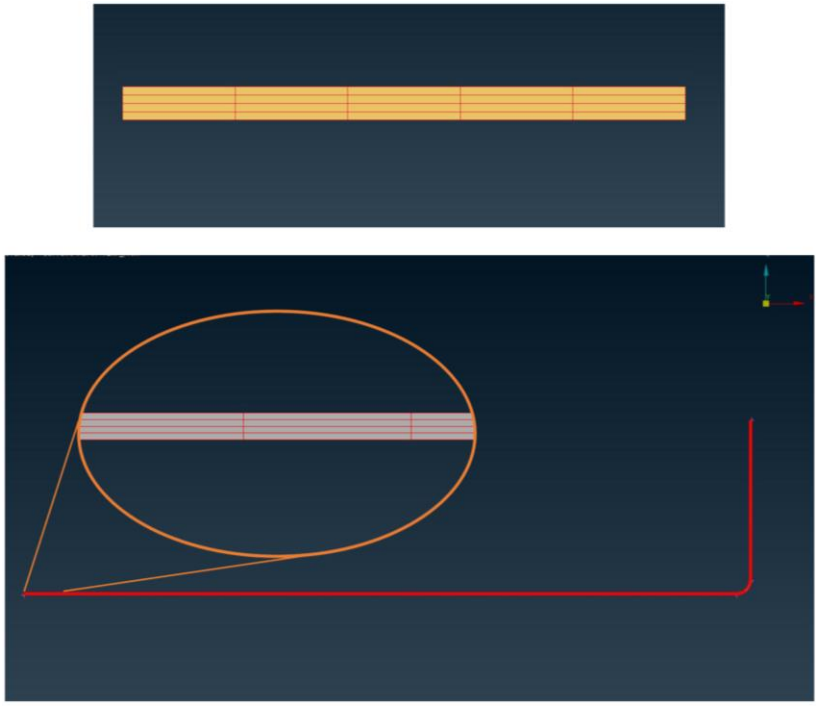

Figure 39: Solids Created Using Extrude Command

A skin of shell elements, around the solid elements is created, to be used for defining contacts in the later stages of test simulation setup. As can be seen from the Figure 39, only one plate is created following all these processes. The plate was multiplied using command 'copy'. For tests, ASTM D1002 and ASTM D1876 the command 'copy' was used and only one copy of the plate was created. For the test ASTM D3528, second plate of 3 mm was created using 'copy' command and the plate of 1.5 mm was created again by using points, then creating surface, followed by extruding the meshed surface to 1.5 mm thickness. At the end, the solids were covered with a layer of shells as the other plates. The shells are used mainly for contact and have 1 mm thickness. Figure 40 shows the material card for shell elements used as skin for solid elements of specimen plate. On the material card '*r*' represents the density of the material. The value of '*r*' used for shell elements is taken $7.85*10^{-6}$ kg/mm^3, same as of steel. '*E*' is Young's modulus and is 210. 'ni' is Poisson's ratio & 'QVM' is Quadratic Viscosity Multiplier set at its default value 1 and '*f0*' is Damping Target Frequency to dampen the frequency of the output. '*f0*' varies from 0.0 to 1.0. For our tests we use '*f0*' as 0.1.

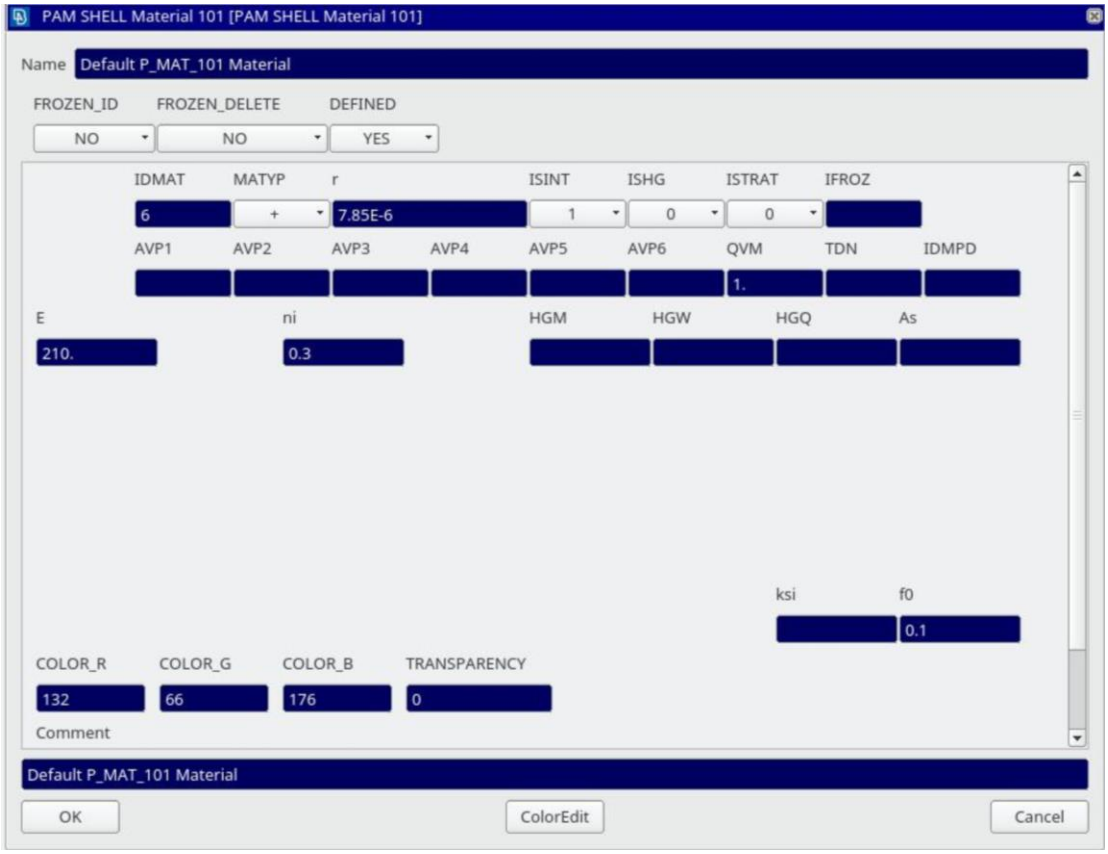

Figure 40: Material Card for Shell Elements

Material card used for solid Steel elements is shown in Figure 41. The density '*r*' is 7.85*10^{-6} kg/mm^3. Shear modulus (Equation 2) '*G*' and bulk modulus '*K*' (Equation 3)are 81.359 GPa and 166.67 GPa.

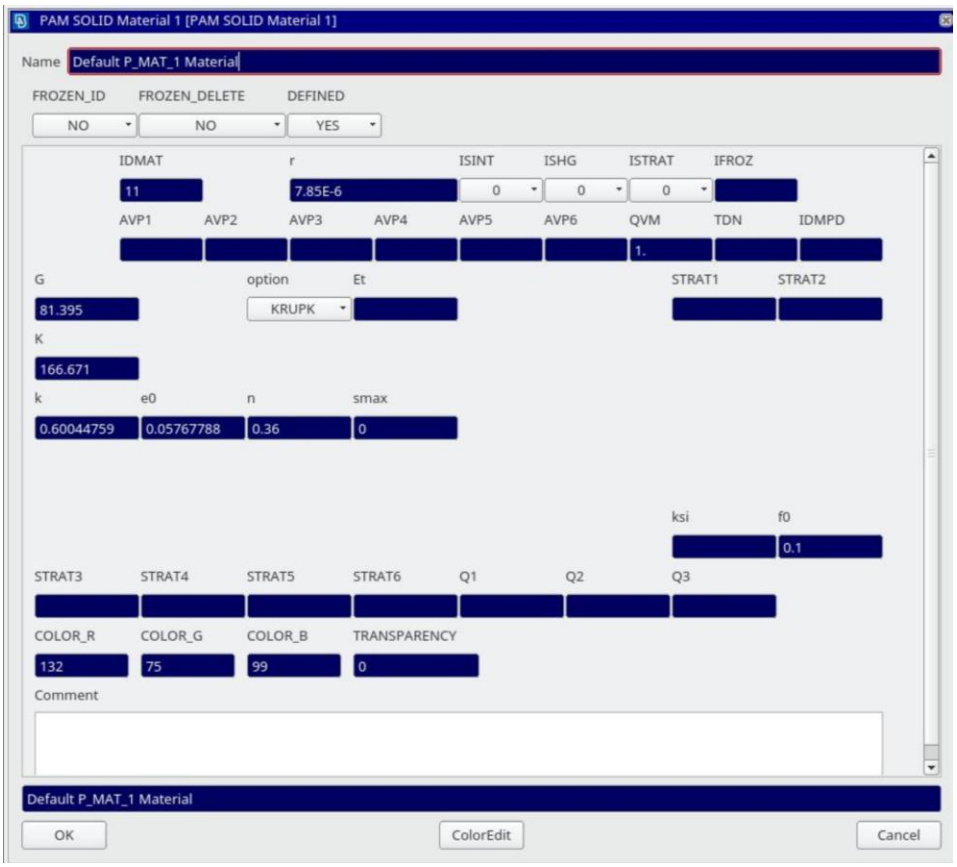

Figure 41: Material Card for Steel Solid Elements

The material card has a provision of choosing from different stress-strain law formulations. For Steel solid elements, in this case, Krupkowsky stress-strain law formulation has been used. It uses the function,

$$\sigma = k\,(\varepsilon_0 + \varepsilon_p)^n.$$

Equation 5: Krupkowsky Stress-Strain Law

Where k, n are hardening coefficients, ε_0 (e0) is offset strain-maximum relative elastics deformation and ε_p (smax)is relative plastic strain. The reason for using this Stress-Strain law formulation is that we don't require to define the stress-strain curve for material, instead two points are sufficient, and the function creates a relevant curve between the points with good accuracy to define the behavior of the material. This law formulation has been used by TÜV SÜD s.r.o. to define material card of Steel.

3.2 CONTACTS

After assigning the materials to the solid and shell elements, they were arranged in 0.2 mm apart from each other with a 12.7 mm overlap for ASTM D1002 (Figure 8) and ASTM D3528 (Figure 9), as per guidelines. For ASTM D1876, the overlap was set to 241 mm (Figure 11). Next step was to create the contact in overlap region between two plates. For this, first the face was created on one of the shell element in the overlap region. Face can be created by selecting the elements on one of the plates in overlap region followed by using the feature 'faces'. Figure 42 shows an example of face created on elements of test ASTM D1876.

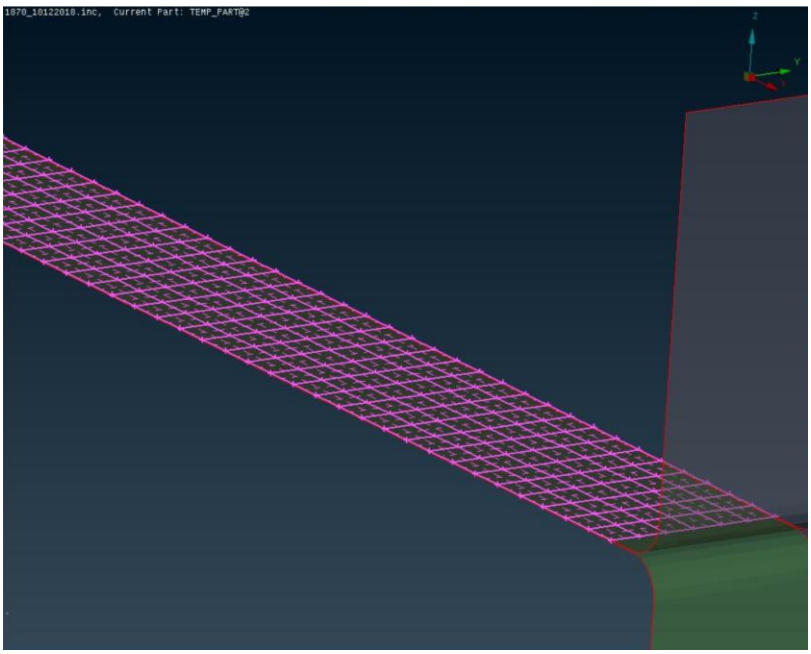

Figure 42: Example of Faces created on ASTM D1876

After positioning of the plates opposite to each other and creating face on one of the side, next step was to create the adhesive contact layer. For this, many approaches were possible, using connection manager to create spot-weld Hexa-Contact was used. Figure 43 shows the connection manager dialogue in ANSA. The connection is created between the skin shells of both the plates. For this process, it is necessary for connection manager to identify an element face, hence the previously created face is used. From the elements of this face, a spot-weld Hexa-Contact is projected to the other plate. As can be seen in Figure 43, the contact created is one layered single contact. The same process was used to create the connection for other two tests. However, in case of ASTM D3528, '*Single Contact*' box was left unchecked as

there were supposed to be two adhesive layers on either side of the 3 mm plate, on the overlap area (Figure 9).

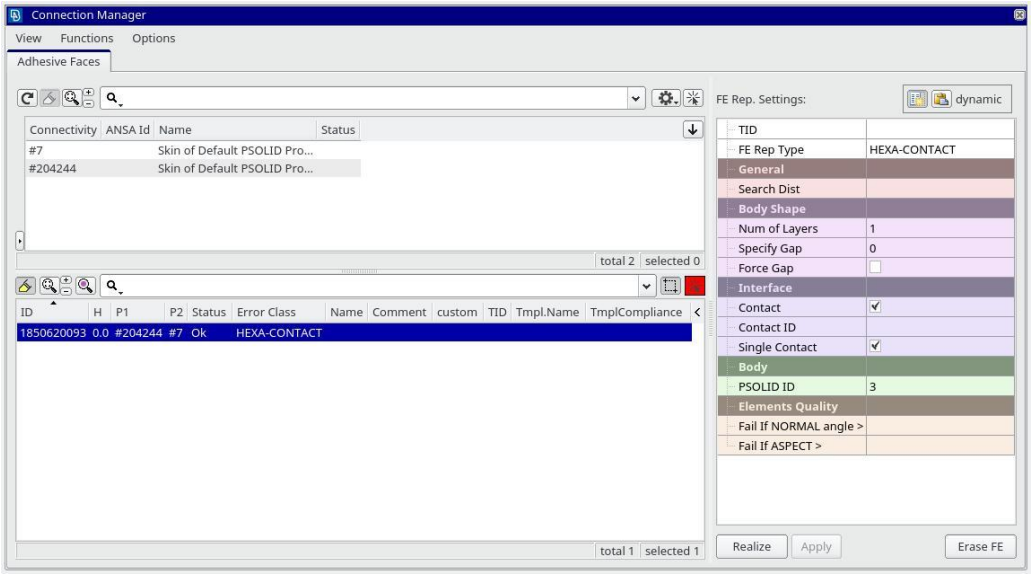

Figure 43: Connection Manager

There are many material types available in PAM-CRASH to define the adhesive material card. As adhesives exhibit hyper-elastic material properties, choosing it would have been an ideal choice. The property and material card used was created for the adhesive. Material card of adhesive can be seen in Figure 45. Material Type 1 in PAM-CRASH is an elastic-plastic model for solid and tetrahedral elements with isotropic and/or kinematic hardening. It was designed to describe the deformation of metallic components during vehicle crashes [22]. Its behaviour under uniaxial loading is equivalent to the mechanical model shown in Figure 44. The decision of using basic Material Type 1 is based on the client's trust on this material type, it has been used for quite some and has been sufficient for their simulations purposes. Ficarra 2011 [18] discusses, in modern adhesives, as the material approaches yield stress adhesive material properties become non-linear. This non-linear behavior affects the actual stress distribution, raising the need for elastic-plastic analysis of the adhesive.

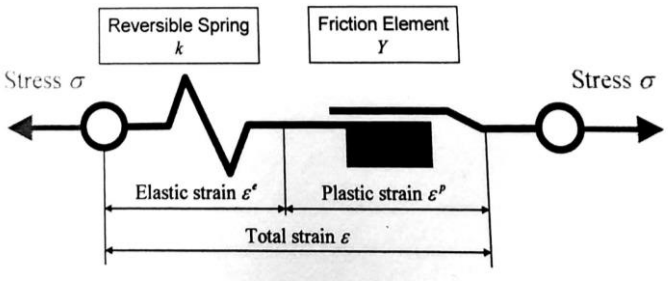

Figure 44: Mechanical Model of Uniaxial Loading [22]

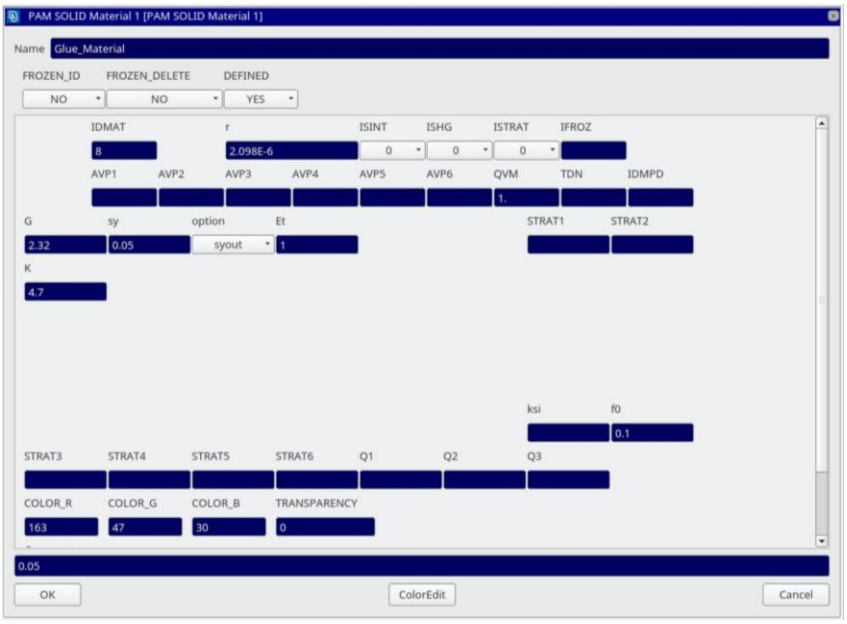

Figure 45: Material Type 1 - Elastic-Plastic Solid with Isotropic and/or Kinematic Hardening

As can be seen in Figure 45, there are different parameters that can be altered to tune the material. '*G*' is shear modulus, '*K*' is bulk modulus, '*SIGMAy*' is yield point, '*f0*' is Damping target frequency and '*et*' is tangent modulus (slope of stress-strain curve). At first the values of these parameters were chosen keeping in mind the properties of the adhesive. Figure 46 shows the spot-weld hexa-contact (represented by red Asterix) created using connection manager dialogue box. Figure 47 shows the adhesive solid elements created between the two plates.

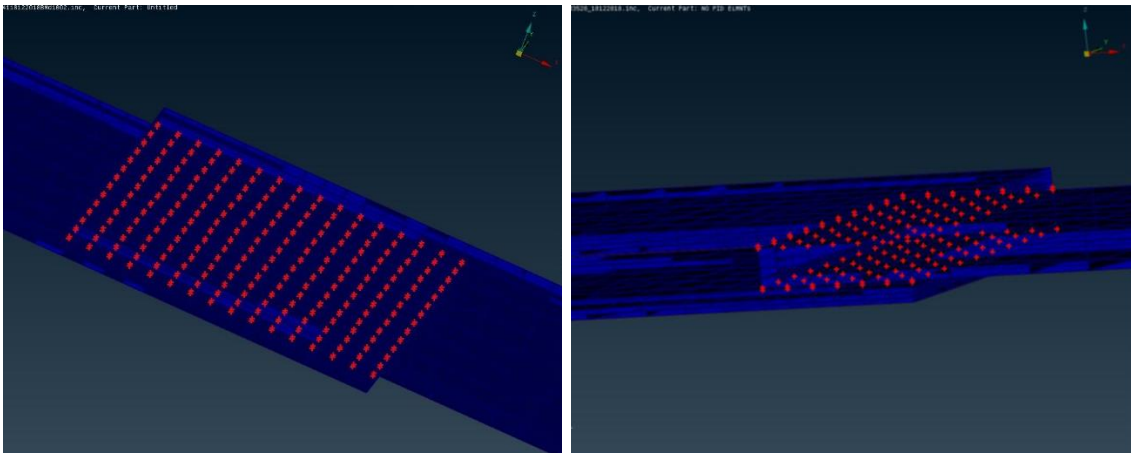

Figure 46: Spot-weld Hexa-Contact ASTM D1002 & ASTM D3528 Test

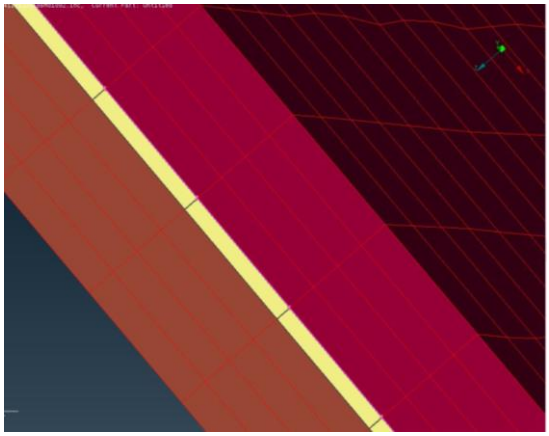

Figure 47: Adhesive Solid Elements

During simulation, as the initial parameter entered for the adhesive, forces generated were so high that it caused the solid plate elements to create negative volume and ultimately result is error. Another type of contact, "anti-collapse" contact, was added to the solid elements of the plates in all the test to avoid the error caused by negative volume created during the simulation. Figure 48 shows the highlighted element with anti-collapse contact. The contact gets activated when the solid elements compress and reach a minimum thickness value of 0.3 mm, the solid gets stiffened and the negative volume is neglected. Anti-collapse is not applied to the solid elements assigned for adhesive because the glue line thickness is 0.2 mm already and is not detectable by anti-collapse contact definition and, we didn't want anti-collapse to be a factor affecting the simulation results by stiffening the adhesive.

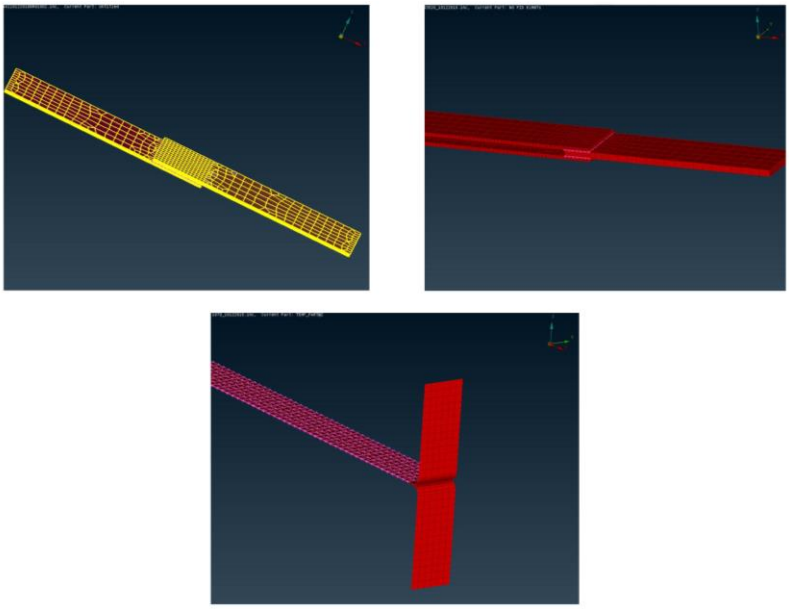

Figure 48: Solid elements Anti-Collapse Contact

3.2 TEST SETUP

Two node sets were created on non-bonded sides of the plates. These nodes sets, then were assigned, one for constraining and one for loading. The highlighted nodes in Figure 49 shows the load node set and constrained node set. The constrained node set is used to constrain the motion of that plate when the load was being applied. Similarly, load node set was used to apply tensile load to the plate.

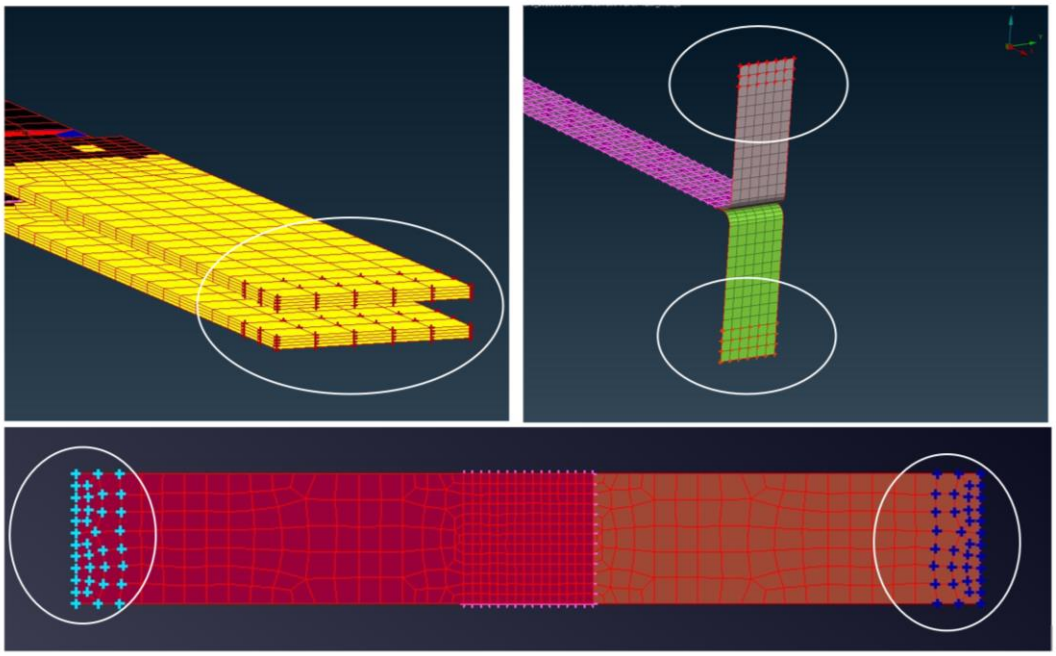

Figure 49: Load Node Set and Constrained Node Set

A sine tensile loading curve on the load node set was applied. The reason behind applying load using a sine wave is that, doing so doesn't put the maximum force on the specimen which could be a very big force and can behave like an impact as the total simulation runs for a few milliseconds. Sine curve loading increases the load gradually. As our main goal was to get the force vs. displacement characteristics of the adhesive, we could run the simulation for milliseconds instead of full 3-4 minutes like physical testing, which could have increased the computation load exponentially. Example of Python loading curve definition can be seen in APPENDIX 1.

To get the information about the displacement, velocity and acceleration of different parts of the specimen, '*THNOD*' (Time history nodes) feature was used. This feature allows to select the nodes, whose test data will be recorded, and can be plotted against time. Figure 50 shows the highlighted nodes selected for time history plots. The nodes are selected on each end of plates and where the adhesive joins with these plates. Our focus was to get the time history plot of node situated at the end of moving cross-head. As we can corelate this node's T-H plot with the physical test readings. A displacement against time curve (ASTM D1002) of the node on the tensile loaded side can be seen in Figure 51.

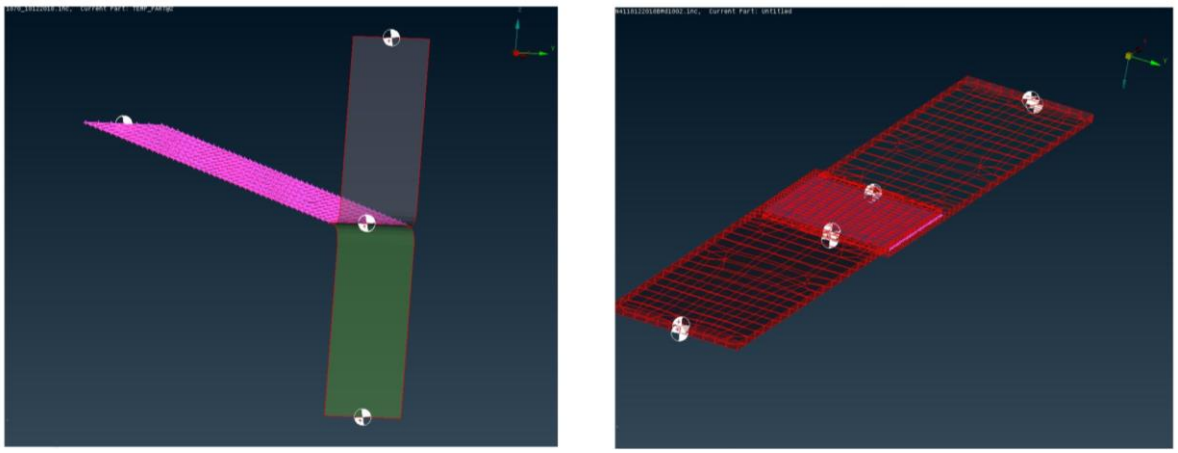

Figure 50: THNOD Nodes ASTM D1876 & ASTM D1002

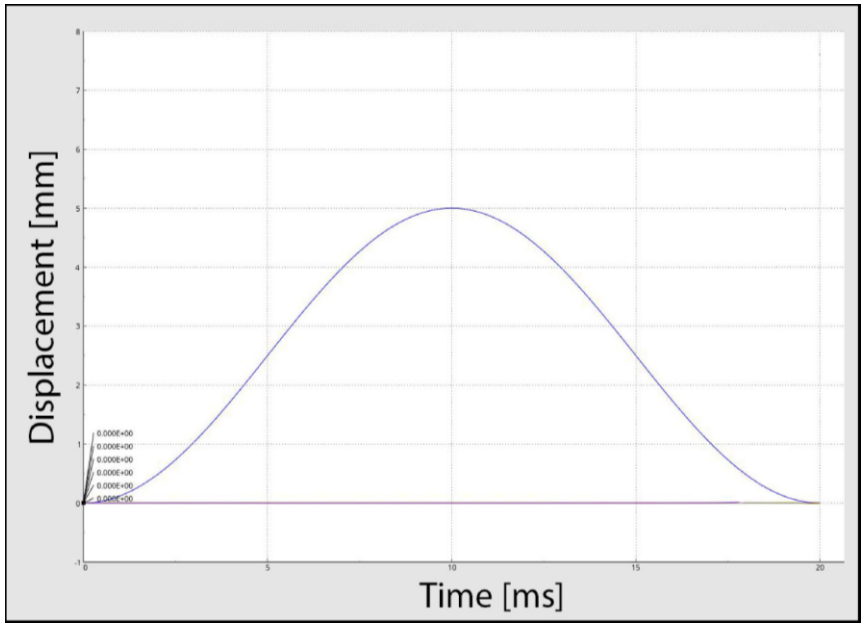

Figure 51: Displacement vs. Time Plot of Node at Tensile Loaded Side

To know the forces in the bonded region, during tensile loading, a feature called '*SECFORC*' is used. There are different definitions to measure the section force. Three node sets were created at different locations of the specimen. To get the force against time graph, we needed to make a node sets on adhesive face and the associated element's set for to be used in combination to define the '*SECTION*'. A similar process was repeated with a node set and element set on the plate. The last node set was used to make a '*SUPPORT*'. The highlighted nodes can be seen in Figure 52.

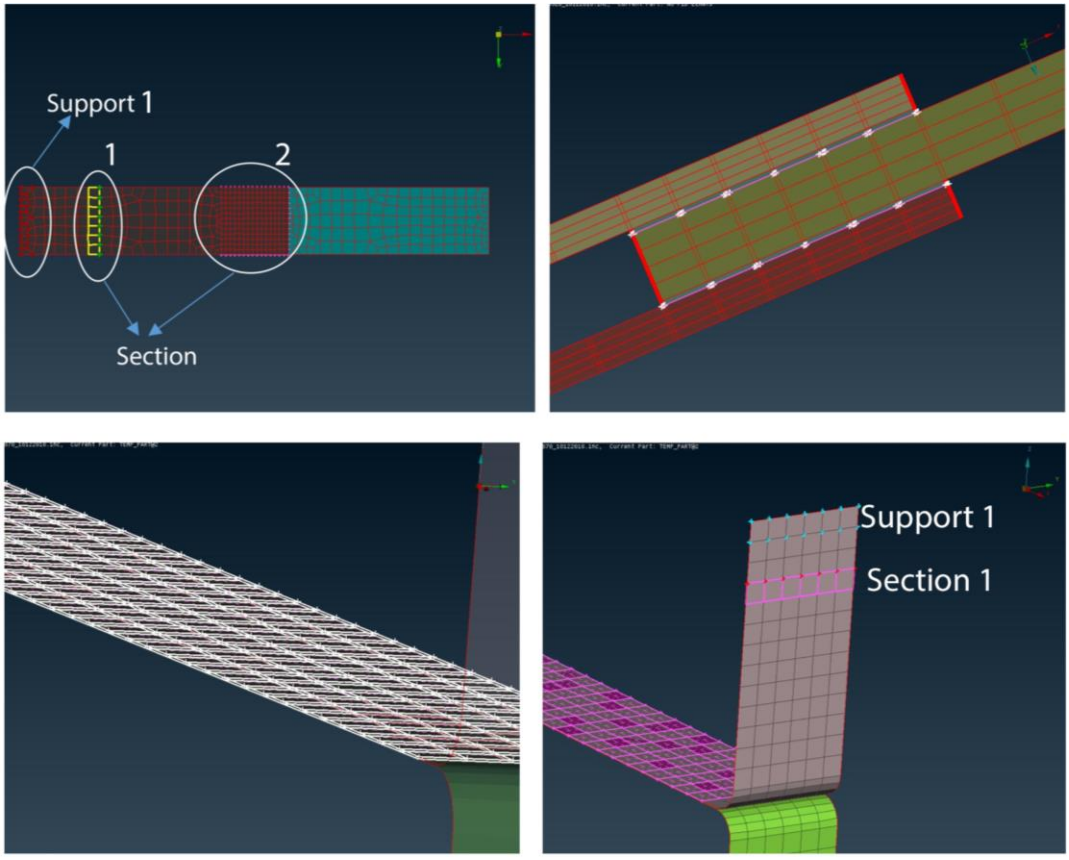

Figure 52: 'SECFORC' Definition

4 FEM SIMULATIONS

4.1 MATERIAL TUNING & SIMULATIONS ASTM D1002

After the test was setup, the next step was to do simulations using the adhesive model and tune it to match the physical testing data. At first, the ASTM D1002 test setup was tested with parameters as shown in Table 1 and then, they are altered one by one to find the right combination.

No.	Young's Modulus *'E'*	Mass Density *'r'*	Poisson's ratio *'v'*	Shear Modulus *'G'*	Bulk Modulus *'K'*	Tangent Modulus *'et'*	Yield Point *'sy'*	Force at 3.75 mm Displacement
#	[GPa]	[kg/mm2]	[-]	[GPa]	[GPa]	[-]	[GPa]	[kN]
1	1.718	2.09	0.31	0.665	1.507	1	0.05	9.869
2	1.718	2.09	0.31	0.665	1.507	50	0.05	Error Termination
3	1.718	2.09	0.31	0.665	1.507	0.5	0.05	9.8
4	1.718	2.09	0.31	0.665	1.507	0.05	0.05	118?
5	1.718	2.09	0.31	0.665	1.507	0.01	0.05	Error Termination
6	1.718	2.09	0.15	0.746	0.818	0.01	0.05	8.885
7	1.718	2.09	0.25	0.687	1.145	0.01	0.05	8.885

Table 3: Glue Material Input Matrix for ASTM D1002; Orange Cells: Input, Red Cells: Error Output, Green Cell: Desired Output

Input values for adhesive material card of ASTM D1002 can be seen in Table 3. These values are chosen out of more than 50 simulation iterations as they are most relevant for our goal and understanding of the adhesive behaviour. As we are already provided with Young's modulus '*E*' and mass density '*r*' by the manufacturer, they were kept constant and other parameters were changed simulation by simulation to see what effect they have on behaviour of the adhesive. Poisson's ratio '*v*' is chosen, since the Poisson's ratio of an incompressible material which deforms elastically on small strain rates is 0.5 (for example, rubber) and as material gets stiffer the Poisson's ratio approaches 0 (for example, cork). The adhesives usually have a Poisson's ration between 0.35 - 0.25. For initial simulations, Poisson's ratio was chosen as 0.31.

Shear modulus '*G*' and bulk modulus '*K*' are related to Poisson's ratio and Young's modulus, as shown in Equation 2 & Equation 3. As the Young's modulus is kept constant at 1.718 GPa, changing Poisson's ratio changes shear and bulk Modulus input values as well. Initial value of tangent modulus '*et*' is kept as 1 and yield point at 0.05 GPa. Force at 3.75 mm displacement is measured across Section 1 (shown in Figure 52) during the physical testing

the material ruptured at 3.75 mm cross head displacement. Section 1 was a logical choice to measure the section force as during the physical testing, the machine measures tensile force at the cross head near the specimen is clamped to the machine, measuring force provided us with more realistic and comparable results.

Initially the Poisson's ration was altered from the value of 0.35 to 0.25 with an increment or decrement of 0.02 from 0.31. Changing Poisson's ratio didn't change the high values of force produced at 3.75 mm displacement. Changing yield point (0.05 GPa – 0.013 GPa) only drops the force at 3.75 mm displacement by only a little and didn't give the desired force.

At last, the tangent modulus was changed from 1 to 50 (Table 3, #2), the simulation resulted in error termination due to collapsing of the steel solids to a negative volume, this indicated the increasing tangent modulus to 50 made the adhesive solids too stiff. Next iteration (Table 3, #3) was performed and the value of '*et*' was taken as 0.5 and the force dropped by 7%. For next simulation (Table 3, #4), the value of '*et*' was taken as 0.05 and the force dropped by 48%. The '*et*' was further reduced to 0.01(Table 3, #5), the simulation ended in error termination due to collapsing of the adhesive solids to a negative volume, this indicates that reducing '*et*' to 0.01 made the adhesive solids too soft. To make them stiffer, the Poisson's ratio was dropped to 0.15 (Table 3, #6) while keeping '*et*' at 0.01, this resulted in normal termination of the simulation and dropped the force to 8.85 kN (desired force) at 3.75 mm displacement of cross head. After this, the Poisson's ratio was increased to 0.25, a more realistic value for adhesives, the force remained the same while also providing enough stiffness to the adhesive elements to not collapse to negative volume.

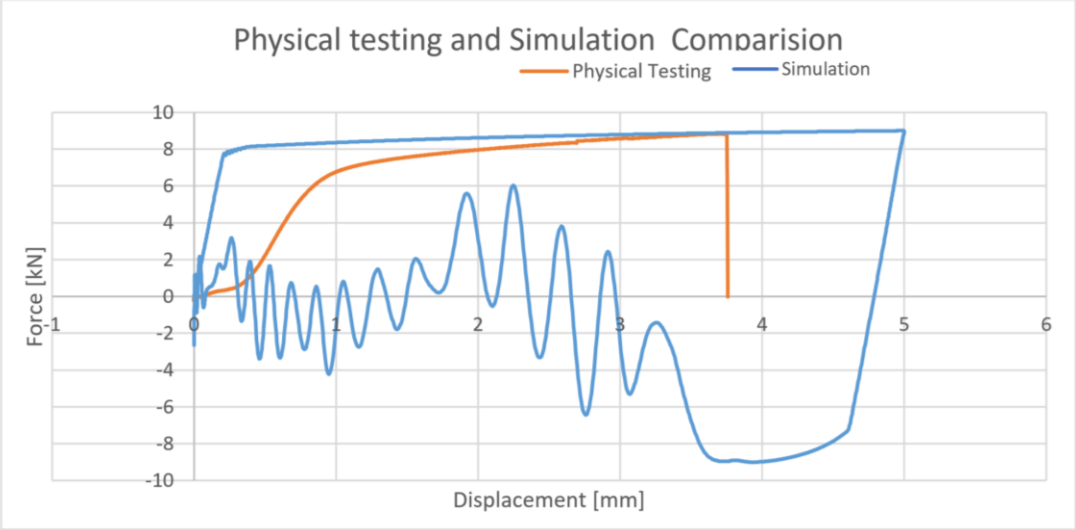

Figure 53: Force vs. Displacement Curves of ASTM D1002 Physical Testing and PAM-Crash Simulation for Simulation #7, Table 3

As can be seen in Figure 53, the curves intersect at 3.75 mm displacement and have same force 8.85 kN. The curve for simulation extends beyond 3.75 mm displacement. Next step was to find a material model which has the provision to define its rupture criteria while maintaining the same properties as Material Type 1 for Pam-Crash. Remaining results of simulations from Table 3 can be seen in Figure 60, APPENDIX 2.

Material Type 16 [22], in PAM-CRASH is an elastic-plastic model for FEM hexahedral, tetrahedral and SPH (Smooth Particle Hydrodynamics) elements. It is designed to describe the deformation of metallic materials during forming and crashes and provide various, yield criteria, hardening laws and failure models. Apart from all the tunable parameters provided by Material Type 1, it gives a provision to input '**EPSIpmax**', maximum plastic strain for material elimination. Material card for Material Type 16 can be seen in Figure 54.

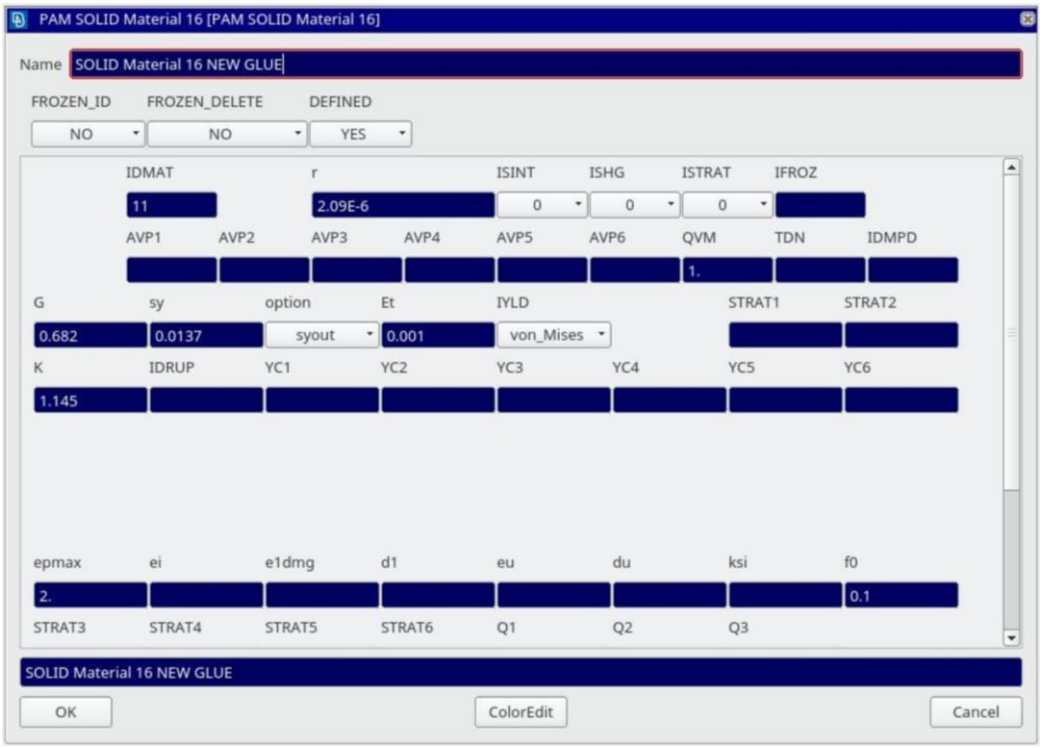

Figure 54: Material Type 16 - Elastic-Plastic with Damage & Failure for Solid Elements and SPH [22]

An element is eliminated from simulation, as soon as equivalent plastic stain values at its integration points has reached the specified limit of elimination [22]. Input matrix for Material Type 16 can be seen in Table 4.

No.	Poisson's ratio 'v'	Shear Modulus 'G'	Bulk Modulus 'K'	Tangent Modulus 'et'	Yield Point 'sy'	Element Elimination 'epmax'	Force at 3.75 mm Displacement	Element Elimination
#	[-]	[GPa]	[GPa]	[-]	[GPa]	[-]	[kN]	[mm]
8	0.25	0.687	1.145	0.01	0.05	10.5	8.85	4.41
9	0.25	0.687	1.145	0.01	0.05	10	8.85	4.21
10	0.25	0.687	1.145	0.01	0.05	9	8.85	3.83
11	0.25	0.687	1.145	0.01	0.05	8.8	8.85	3.75

Table 4: Material Type 16 Input Matrix for ASTM D1002; Orange Cells: Input, Red Cells: Error Output, Green Cell: Desired Output

As can be seen in Table 4, the orange color highlighted cells correspond to the input variables. All the parameters are kept same as the simulation #7(Table 3), with an additional variable '*epmax*' which was varied to define the rupture criteria and element elimination for the material model. The value of '*epmax*' is usually higher than 0. For the first few simulations the was kept from 0.02 – 5, as they didn't have any impact on results, the value was increased to 12 and then brought down to the input values shown in Table 4 were most relevant for our desired output. As can be seen in simulation #8 (Table 4), the elements reached their rupture limit at 4.41 mm crosshead displacement. The value of '*epmax*' is reduced further to 10, it leads to decrease the displacement of element elimination from 4.41 mm to 4.21 mm. The value of '*epmax*' was then further reduced in two steps and 8.8 (simulation #11) was the value of '*epmax*' when element elimination occurred at 3.75 mm. Element elimination action of the adhesive solid elements can be seen in Figure 55.

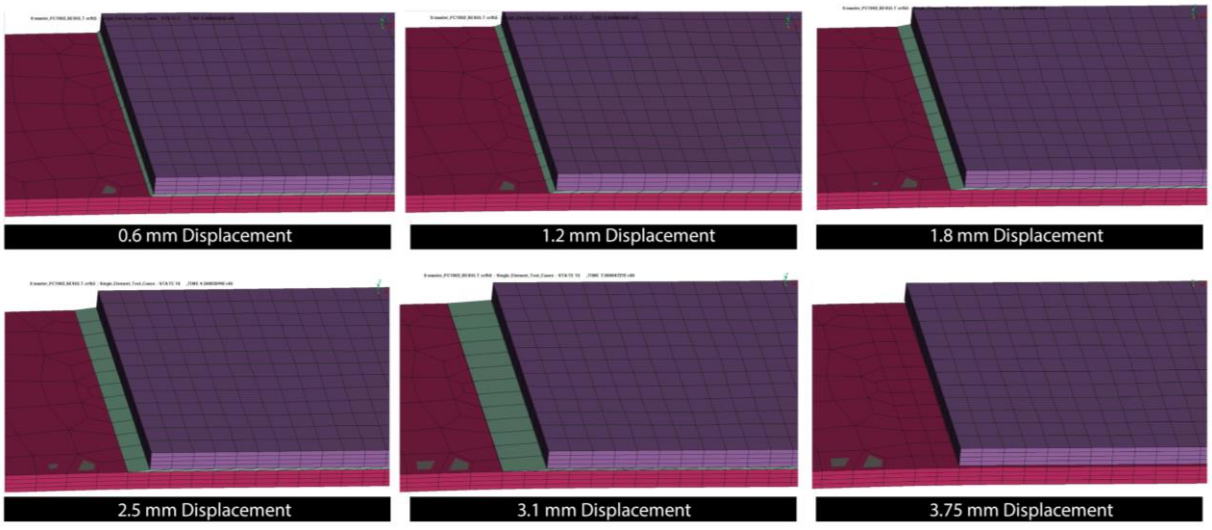

Figure 55: ASTM D1002 Simulation Animation and Element Elimination (Simulation #11)

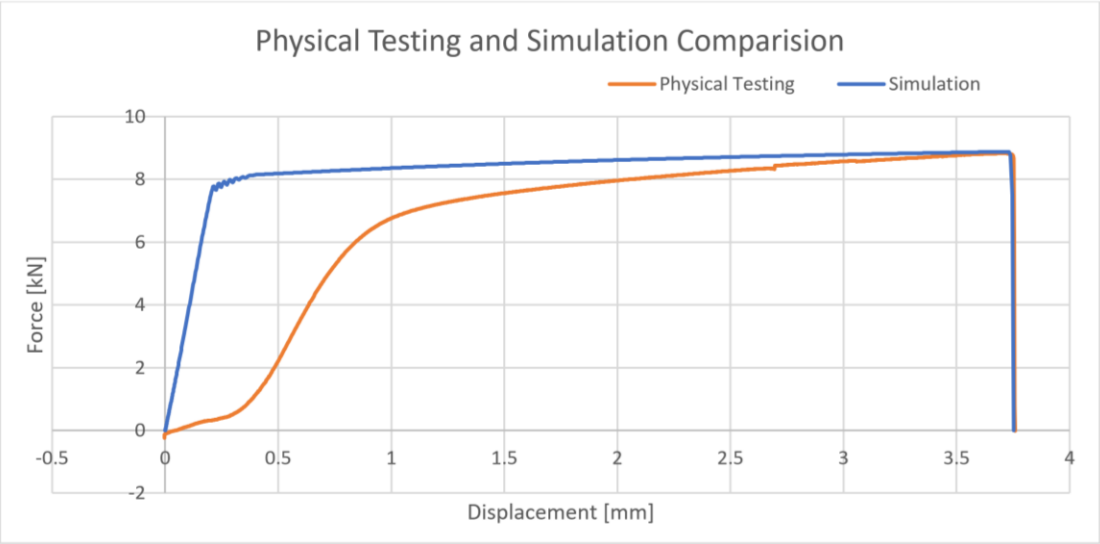

Figure 56: Force vs. Displacement curves of ASTM D1002 Physical Testing and PAM-Crash Simulation #11 with Rupture Model, Table 4

Figure 56, shows the graph of force vs. displacement curves of ASTM D1002 physical testing and PAM-CRASH simulation for simulation #11, Table 4. The material model meets the failure force and rupture criteria compared to physical testing data. Remaining results of simulations from Table 4 can be seen in Figure 61, APPENDIX 2.

4.2 MATERIAL TUNING & SIMULATIONS ASTM D3528

After the tuning of Material Type 16 for ASTM D1002 test simulation the same material card was applied to the double lap shear test simulation. The input matrix can be seen in Table 5.

No.	Poisson's ratio *'v'*	Shear Modulus *'G'*	Bulk Modulus *'K'*	Tangent Modulus *'et'*	Yield Point *'sy'*	Element Elimination 'epmax'	Force at 5.3 mm Displacement	Element Elimination
#	[-]	[GPa]	[GPa]	[-]	[GPa]	[-]	[kN]	[mm]
1	0.25	0.687	1.145	0.01	0.05	10.5	17.81	4.19
2	0.25	0.687	1.145	0.01	0.05	12	17.9	4.76
3	0.25	0.687	1.145	0.01	0.05	13	Error Termination	Error Termination
4	0.15	0.746	0.818	0.01	0.05	12.5	Error Termination	Error Termination
5	0.15	0.746	0.818	0.01	0.05	12	17.9	4.76

Table 5: Material Type 16 Input Matrix for ASTM D3528; Orange Cells: Input, Red Cells: Error Output, Green Cell: Acceptable Output

As can be seen in Table 5, the input values that which created accurate output, did not give desired output for double lap shear test. Further investigation was done by changing '*epmax*' to 12 (simulation #2), The rupture criteria and failure for improved and moved towards the desired values. '*epmax*' was further increased to 14, resulted in error termination of the simulation due to negative volume of adhesive solids. Further steps were, slowly decrease the '*epmax*' and increase the stiffness of the material to see if they don't result in negative volume beyond 4.8 mm displacement, the stiffness was increased by lowering the Poisson's ratio from 0.25 to 0.15. As can be seen in simulation #4 (Table 5), at 0.15 Poisson's ratio and 12.5 '*epmax*', resulted in error termination. The value of '*epmax*' was reduced back to 12 and Poisson's Ration 0.15 in simulation #5 (Table 5), the result came out to be similar to Simulation #2 in Table 5. Figure 57, shows force vs. displacement curves of ASTM D3528 physical testing and PAM-CRASH simulation for simulation #2, Table 5. Remaining results of simulations from Table 5 can be seen in Figure 62, APPENDIX 2.

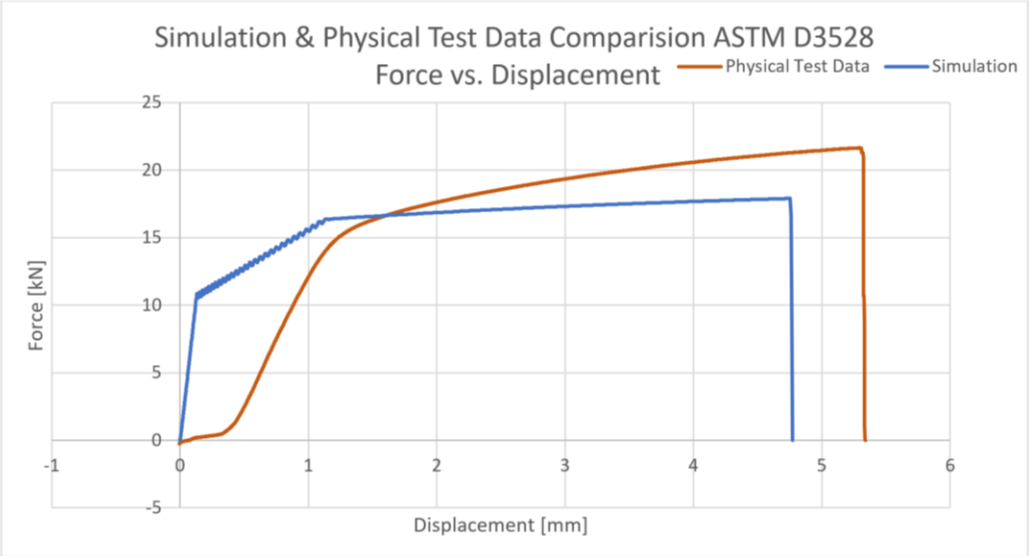

Figure 57: Force vs. Displacement Curves of ASTM D3528 Physical Testing and PAM-Crash Simulation for Simulation #2, Table 5

Element elimination action of the adhesive solid elements can be seen in Figure 58.

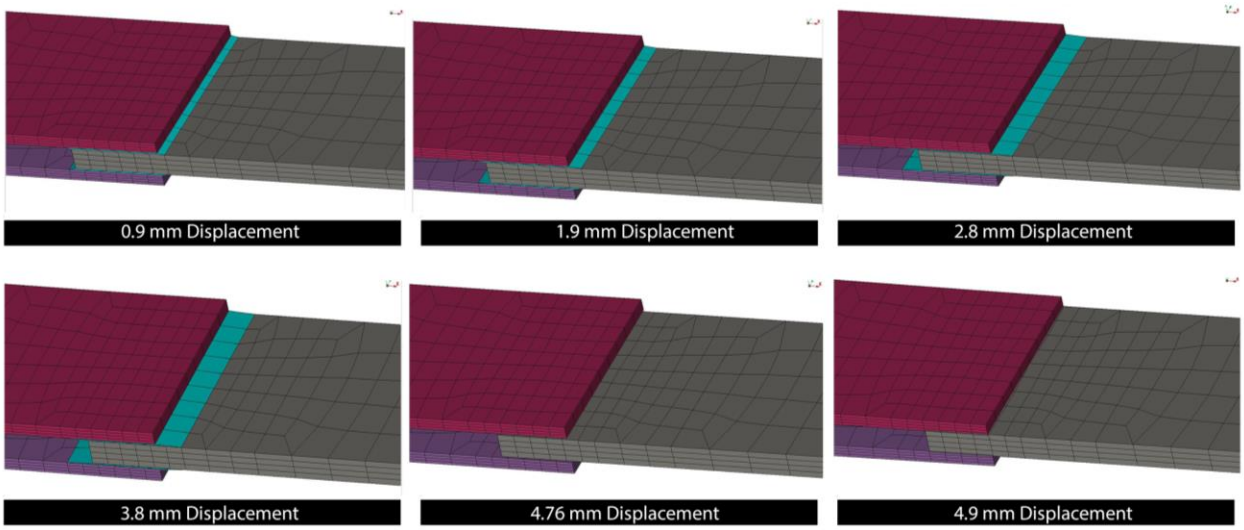

Figure 58: ASTM D3528 Simulation Animation and Element Elimination (Simulation #2)

4.3 MATERIAL TUNING & SIMULATIONS ASTM D1876

After the tuning of Material Type 16 for ASTM D1002 and ASTM D3528 test simulation the same material card was applied to the peel test simulation. The input matrix can be seen in Table 6: Material Type 16 Input Matrix for ASTM 1876; Orange Cells: Input, Red Cells: Error Output, Green Cell: Acceptable Output, Table 6.

No.	Poisson's ratio *'v'*	Shear Modulus *'G'*	Bulk Modulus *'K'*	Tangent Modulus *'et'*	Yield Point *'sy'*	Force at 3.75 mm Displacement	Element Elimination
#	[-]	[GPa]	[GPa]	[-]	[GPa]	[kN]	[mm]
1	0.25	0.687	1.145	0.01	0.05	Error Termination	Error Termination
2	0.15	0.746	0.818	0.01	0.05	Error Termination	Error Termination
3	0.1	0.780	0.715	0.01	0.05	Error Termination	Error Termination

Table 6: Material Type 16 Input Matrix for ASTM 1876; Orange Cells: Input, Red Cells: Error Output, Green Cell: Acceptable Output

For peel test simulation, many different iterations were done, all the possible combinations tried, as were tried for ASTM D1002 and ASTM D3528 material card tuning. Material Type 16, was unable to perform peel test as the adhesive solid elements collapsed as the elements stretch in normal (z-direction) and compresses in longitudinal direction (x-direction). Figure 59 shows the visualization of the ASTM D1876 simulation.

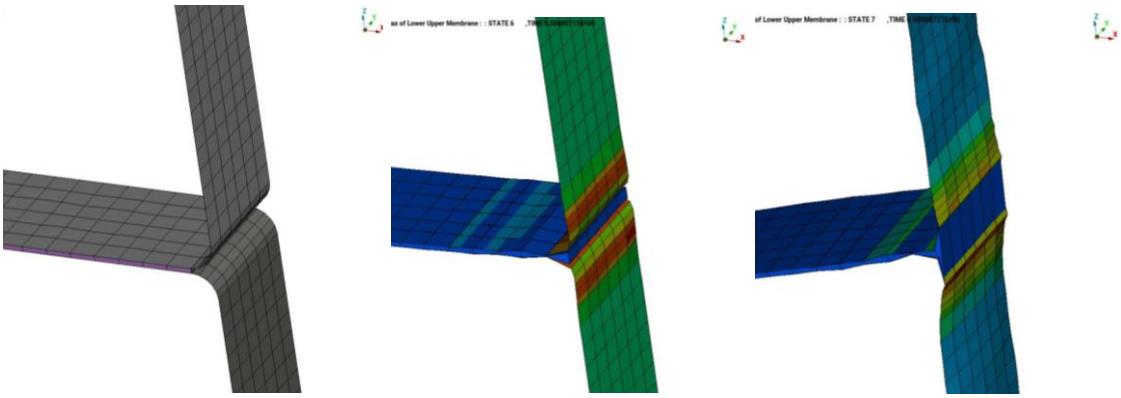

Figure 59: ASTM D1876 Simulation Visualization

5 DISCUSSIONS

The simulation results of three different tests show different results. Material Type 16 performs well in the case of single lap shear test. As the model was first tuned to match the stiffness and rupture criteria of single lap shear test data from physical test, it was expected to create very promising results. The model shows an error of 0.5%. It was found that, the main parameters which drastically change the material model behavior are Poisson's ratio and tangent modulus. And their respective values at which the material matched the physical testing data are 0.25 and 0.01. The value of '*epmax*' to match rupture criteria is found to be 8.8.

It can be said, that the material model for Material Type 16, in case of ASTM D3528 test is able to achieve 82.3% of the force in comparison with physical test data, when applied with the same parameters as applied to single lap shear test simulation. The material also ruptures at 4.19 mm instead of desired 5.3 mm displacement. This can be explained by the fact that the simulation is based on the idealized test scenarios, there could be many factors affecting the physical testing results. The physical testing's force vs. displacement curve is an average taken from 7 different readings, these readings had a big range of variations, hence the averaged curve is not so reliable.

For ASTM D1876 simulation, there were no results produced as the material collapsed and resulted in negative volume of the adhesive solid elements. Figure 59 shows the accurate representation of the phenomena.

6 CONCLUSIONS

The project dealt with the investigation of types of adhesive and their important properties. This was followed by choosing an epoxy resin-based adhesive which is used for industrial applications. Loctite EA 9466, was an accurate choice as it is also used by TÜV SÜD s.r.o. and its data sheet provided the necessary parameters needed to proceed with the physical testing and later for modelling the material model. It was followed by choosing the standard guideline tests for the physical testing and ASTM D1002 (single lap shear test), ASTM D3528 (double lap shear test) and ASTM D1876 (peel test) were chosen and performed successfully, the test data was acquired in the form of force vs displacement curves.

The physical tests were setup on the FE pre-processor software ANSA, the adhesive material model (Material Type 16) was defined and simulated on PAM-CRASH, ASTM D1002 at first. The data collected was compared to the physical test data and tuned iteration by iteration to match the physical test data. The material behavior (stiffness and failure criteria) was match accurately and successfully, with only 0.5 % error. Important parameters to tune an adhesive model are *Poisson's ratio*, *tangent modulus* and *epmax* as can be seen from the input matrix tables.

ASTM D3528 simulation model results for this material were satisfying with 82.3% accuracy. The error is justified by the fact that the simulation is an idealized scenario and the physical test data is an average, the readings showed a large variation and the averaged curve is not 100% reliable. Furthermore, Material Type 16 is not capable to be implemented in peel test (ASTM D1876) scenarios as it results in collapsing and error termination.

This research provides a reliable material model for single lap shear test and double lap shear test scenarios. It also gives an insight of important key points (cutting method, surface preparation and test setup) for performing physical tests and important parameters that are crucial for modelling and tuning adhesive FE material model.

This study can be used for performing simulations which require an adhesive FE material model. It can further be extended in future and more work can be done to improve the material model for peel test simulation by using the material cards and knowledge from this research, hyper-elastic material models can be explored.

REFERENCES

[1] P. Mechanics, "Popular Mechanics," [Online]. Available: https://www.popularmechanics.com/home/how-to/a5754/how-to-free-a-rusted-bolt/.

[2] Wonkeedonkeetools, "Wonkeedonkeetools," [Online]. Available: https://www.wonkeedonkeetools.co.uk/rivets/a-brief-history-of-rivets.

[3] S. E. Fastening, "Stanley Engineered Fastening," [Online]. Available: https://www.stanleyengineeredfastening.com/product-brands/pop/pop-rivet-selection-factors.

[4] Adhesives.org, "History of Adhesives," [Online]. Available: www.adhesives.org.

[5] ASI, "A Look into Epoxy and Other Types of Adhesives Used in the Automotive Industry," Adhesive Systems, Inc., [Online]. Available: http://instantca.com/a-look-into-epoxy-and-other-types-of-adhesives-used-in-the-automotive-industry/.

[6] A.J.Kinloch, Durability of Structural Adhesives, Applied Science Publishers LTD 1983, 1986.

[7] S. Ebnesajjad, Handbook of Adhesives and Surface Preparation: Technology, Applications and Manufacturing, 2010.

[8] ASTM, *ASTM D1002 - Standard Test Method for Apparent Shear Strength of Single-Lap-Joint Adhesively Bonded Metal Specimen By Tension Loading.*

[9] ASTM, *ASTM D1876 - Peel Resistance of Adhesives (T-Peel Test).*

[10] ASTM, *ASTM D3528 - Standard Test Method for Strength Properties of Double Lap Shear Adhesive Joints by Tension Loading.*

[11] J. V. J. K. P. Z. Michal Zelenek, "COMPARISON OF SURFACE ROUGHNESS QUALITY CREATED BY ABRASIVE WATER JET AND CO2 LASER BEAM CUTTING".

[12] A. Akkurt, "Surface properties of the cut obtained by different cutting methods from AISI 304 Stainless Steel Material," 2009.

[13] A. GmbH, *Arcotest Test Inks Data Sheet.*

[14] TechTest, *Recognoil 2W datasheet.*

[15] Kraintek, "Ultrasonic cleaning," Kraintek Czech s.r.o., [Online]. Available: https://www.kraintek.cz/ultrazvukove-cisteni.

[16] Henkel, "Loctite EA 6466 Datasheet," [Online]. Available: https://proprumysl.cz/soubory/221/Loctite-9466-technicky-list.PDF.

[17] R. D. S. G. &. L. F. M. d. Silva, "Advances in Numerical Modelling," 2012.

[18] F. C. Helene, "Analysis of Adhesive bonded fiber-reinforced," 2011.

[19] J. Korta, "Modeling of adhesive bonds using the Finite Element Method," Poland.

[20] A. Spaggiari, "EFFICIENT MODELLING OF COMPLEX ADHESIVELY BONDED STRUCTURES BY STANDARD FINITE ELEMENT TECHNIQUES".

[21] TWI, "Stress-Strain Behaviour of Adhesive," [Online]. Available: https://www.twi-global.com/technical-knowledge/faqs/faq-what-stress-strain-behaviour-can-i-expect-adhesives-to-have.

[22] ESI-Group, Virtual Performance Solution, Solver Reference Manual, 2014.

APPENDIX 1

```
----,----+----o
$ PYTHON VARIABLE DEFINTION
$---+----1----+----2----+----3----+----4----+----5----+----6----+
----7----+----8
PYVAR /  1
NAME LOADING PARAMETER
# Define end time of simulation
T_END  = 20.001
T_MID  = T_END/2
# Define max. deformation
DISP   = 5.0
# Define nb.of complete load/unload cyles
NCYCLE = 1
END_PYVAR
$
PYFUNC/ 1
NAME SINUS LOADING CURVE
#
def sinLoadFunc(t):
  pi = 3.141592654
  y  = <DISP> * 0.5*(sin((t*pi/(<T_END>/(2*<NCYCLE>))-pi/2))+1)
  return y
#
F = sinLoadFunc(X)
END_PYFUNC
$
```

APPENDIX 2

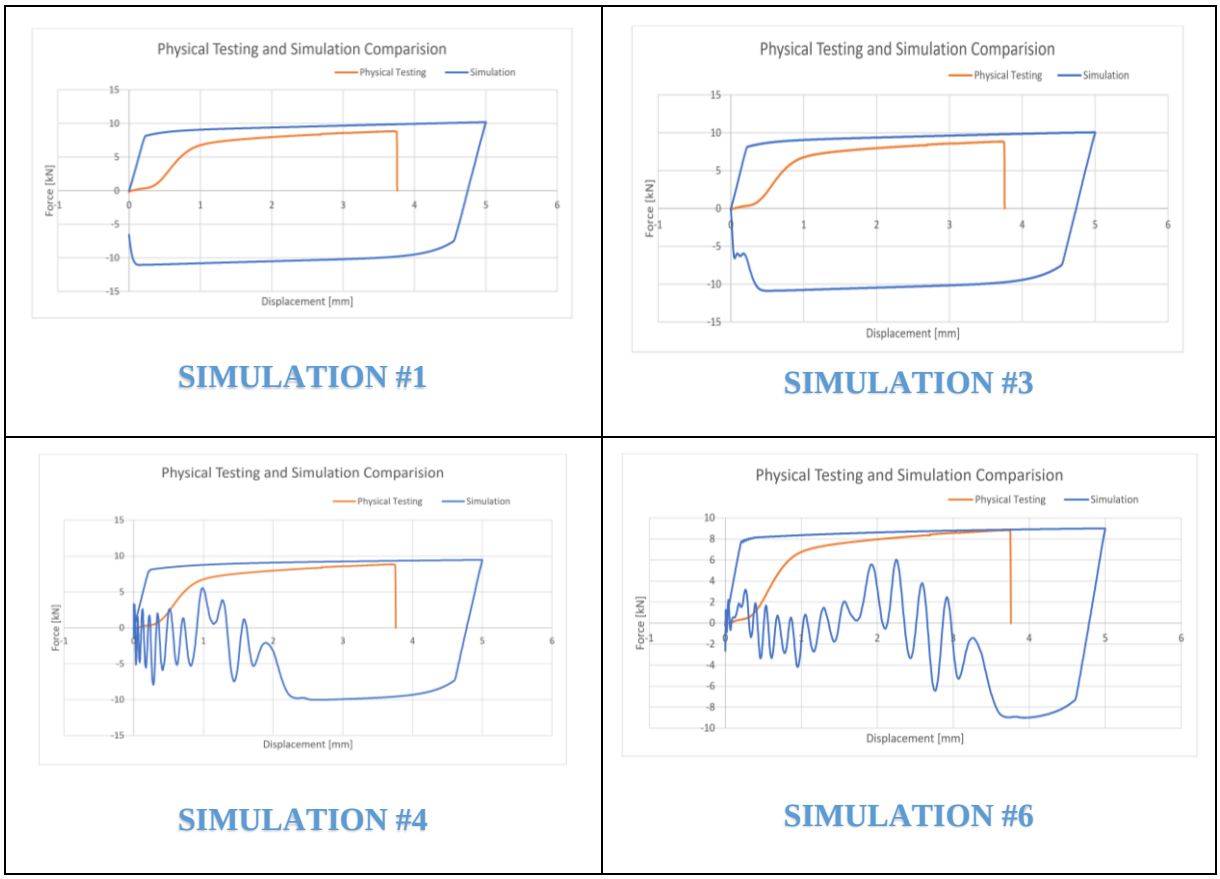

Figure 60: Force vs. Displacement Curves of ASTM D1002 Physical Testing and PAM-Crash Simulation, Table 3

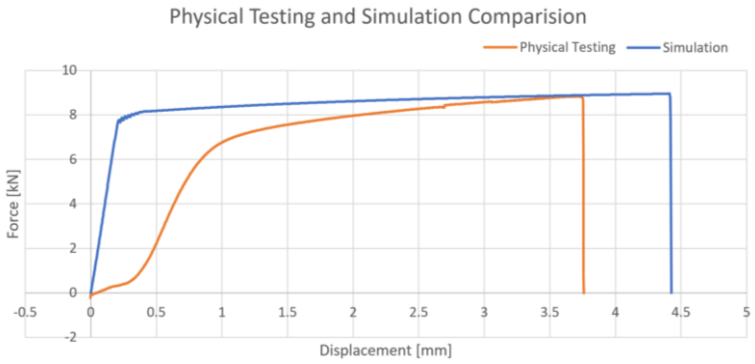

SIMULATION #8

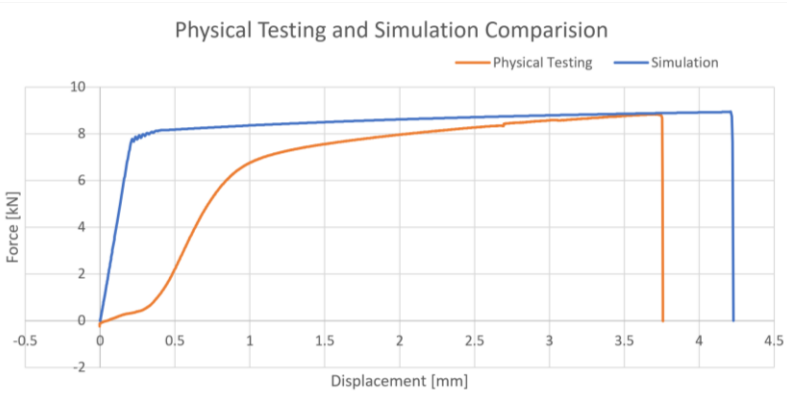

SIMULATION #9

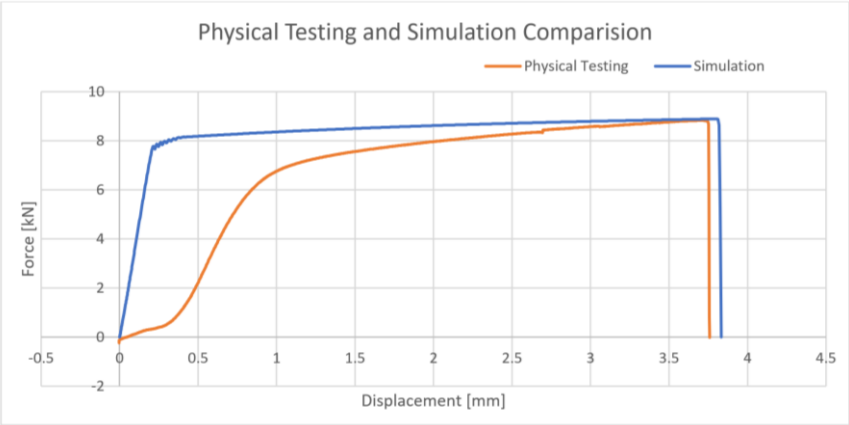

SIMULATION #10

Figure 61: Force vs. Displacement curves of ASTM D1002 Physical Testing and PAM-Crash Simulation with Rupture Model, Table 4

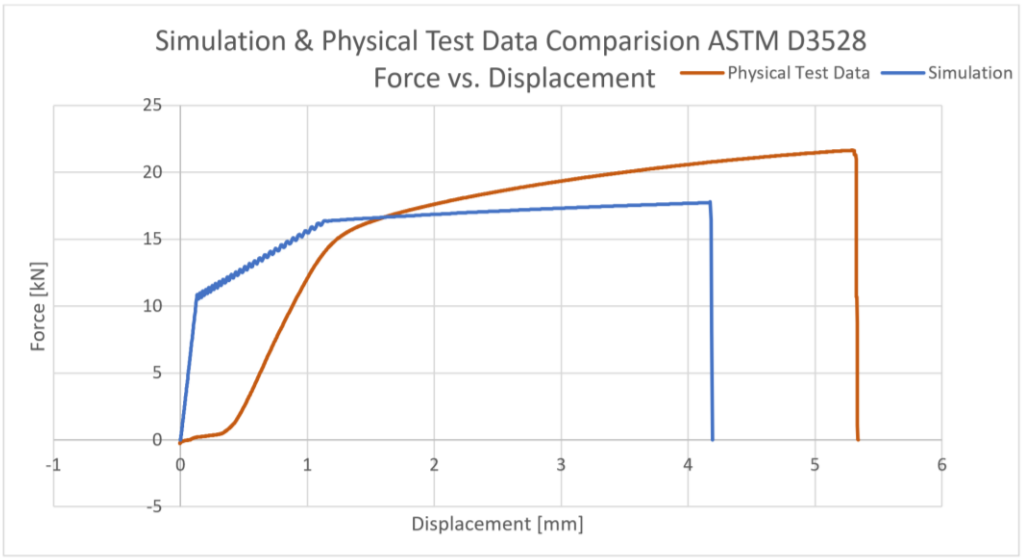

SIMULATION #1

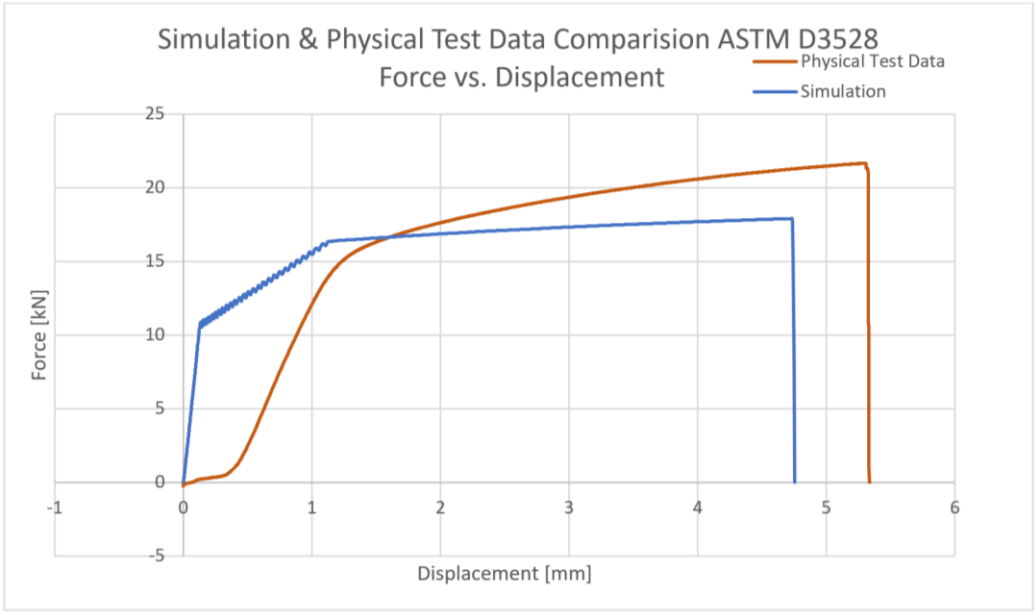

SIMULATION #5

Figure 62: Force vs. Displacement Curves of ASTM D3528 Physical Testing and PAM-Crash Simulation with Rupture Model, Table 5

CONTENTS OF CD

- THESIS REPORT
- PHYSICAL TESTING DATA
- PAM-CRASH SIMULATION MODEL
- PAM-CRASH RESULT